Decoherence of a two-path system by infrared photons

Colby DeLisle [1,2,*] and P. C. E. Stamp [1,2,3,†]

[1] *Department of Physics and Astronomy, University of British Columbia, 6224 Agricultural Rd., Vancouver, B.C., Canada V6T 1Z1*

[2] *Pacific Institute of Theoretical Physics, University of British Columbia, 6224 Agricultural Rd., Vancouver, B.C., Canada V6T 1Z1*

[3] *Theoretical Astrophysics, Cahill, California Institute of Technology, 1200 E. California Boulevard, MC 350-17, Pasadena, California 91125, USA*

(Received 15 May 2024; accepted 3 July 2024; published 26 August 2024)

We calculate the decoherence caused by photon emission for a charged particle traveling through an interferometer; the decoherence rate gives a quantitative measure of how much "which-path" quantum information is gained by the electromagnetic field. We isolate the quantum information content of both leading and subleading soft photons, and show that it can be extracted entirely from information about the end points of the particle's paths. When infrared dressing is used to cure the infrared divergences in the theory, the leading-order soft photons then give no contribution to decoherence, and carry no quantum information. The subleading soft photons in contrast may carry finite which-path information, and the subleading contribution to decoherence takes an extremely simple, time-independent form depending only on the size of the interferometer. An interesting open question is whether or not dressing should also be applied at subleading order; we discuss the possibility of answering this question experimentally.

DOI: 10.1103/PhysRevA.110.022223

I. INTRODUCTION

Our subject in this paper is the well-known "two-path" problem in quantum mechanics [1], in the present case for a charged particle coupled to the electromagnetic (EM) field. We thus assume a pointlike particle with electric charge e, which is traveling through an interferometer, and is put into a superposition of trajectories falling into two distinct classes [2], which we label L and R. We will sometimes refer to this particle as an electron, although it could of course be some other charged particle of larger mass.

An external observer then has the choice of either (i) measuring which path the particle has followed, or (ii) letting it simply pass through the interferometer unmolested by any measuring system. As is well known, in the former case no interference is seen between the two paths, whereas in the latter case, a standard interference pattern is seen on any screen which intercepts the two paths.

However, it is also well known that on its way through the interferometer, the particle couples to the electromagnetic (EM) field, which may be either at temperature $T = 0$ (in its ground state) or at finite T in the rest frame of the interferometer. In either case, the EM field is able to, in effect, passively "measure" which path the particle has followed; in quantum-information-theoretic language, it can act as a "witness" as to which path is followed. This mechanism is of course quite general, and is usually called "environmental decoherence" [3–6]; because of it one expects partial or total destruction of the interference between the two paths.

The particular case of decoherence for two-path systems in which electrons couple to photons has been repeatedly discussed in the literature [7–9]. In this paper we wish to revisit this topic, and clarify the role of low-frequency infrared (IR) photons in bringing about the decoherence. Our aim is to unravel the different contributions, from leading and subleading soft-photon modes, to the decoherence. Inevitably, this requires us to discuss how to deal properly with the infrared divergences present in QED. At the same time we want to understand how the leading and subleading soft contributions might be observable in experiments. This turns out to be difficult because they are often swamped by decoherence from other sources in any realistic experiment.

A. Soft photons and IR divergences

The topic of IR divergences, and their influence on quantum electronic dynamics, of course has a long history, dating all the way back to the work of Bloch and Nordsieck [10]. Early work clarified the ways in which the leading divergences coming from radiative corrections to scattering processes [10–12] were canceled by divergences from virtual soft particles, leading to the derivation of multiplicative "soft factors" (see, e.g., Refs. [13–15], and also Refs. [16–19]) in scattering processes. These factors, when correctly handled, give finite multiplicative corrections to scattering cross sections.

One can write soft factors for any electron-photon scattering process. Here we are interested in the three-point electron-photon scattering process (see Fig. 1), in which the incoming state is an electron with 4-momentum p^a, and the outgoing state is an electron and a photon, with momenta $p^a - q^a$ and q^a, respectively. The "soft-photon theorem" then

*Contact author: delislecolby@gmail.com

†Contact author: stamp@phas.ubc.ca; stamp@tapir.caltech.edu

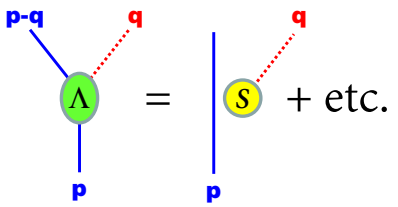

FIG. 1. The three-point electron-photon vertex $\Lambda(p, q)$ written, for small $|\mathbf{q}|$, as a product of the single-electron propagator $K_2(p)$ and the "soft factor" $\mathcal{S}(q)$; compare Eq. (1) in the text.

says that one can write the fully renormalized vertex for this process in the form

$$\Lambda(p, q) \;=\; K_2(p)\,[\mathcal{S}_{(0)}(q) + \mathcal{S}_{(1)}(q)] \;+\; O(|\mathbf{q}|), \qquad (1)$$

where $K_2(p)$ is the fully renormalized two-point propagator for the electron alone, with no photon emission. Here the divergent leading soft factor $\mathcal{S}_{(0)}(q) \sim O(1/|\mathbf{q}|)$, where $\mathbf{q}$ is the 3-momentum, and the subleading factor $\mathcal{S}_{(1)}(q)) \sim O(1)$.

Later work has shown that this result can also be understood as a consequence of asymptotic symmetries [20–22], or by using either an eikonal analysis [23–25] or a coherent state representation for the coupled electron-photon system [26–31]. The latter representation, in which the system is represented by "dressed" electron states, is quite illuminating, for two reasons.

(1) First, dressed states are physically intuitive. As discussed by, e.g., Faddeev and Kulish [31], asymptotic states used in scattering calculations should not be chosen to represent electrons which are totally decoupled from the Maxwell field. Since electromagnetic interactions are long range, electrons are at no point ever "undressed." One should instead always work with dressed states, which represent electrons accompanied by a cloud of low-energy photons. This prescription has consequences when trying to calculate decoherence: the decoherence rate one finds will generally diverge if one evaluates scattering processes between the usual Fock states, but will be convergent if one instead uses dressed states [32,33].

(2) Second, the coherent state representation affords a nice way of separating the leading contributions to the scattering processes from all subleading contributions, first discussed in perturbative calculations [34–37] (this separation is also done in a very clear way in the eikonal expansion [23,24]).

The separation of terms will be crucial in what follows since one question we wish to address here is whether IR dressing should be applied at both leading and subleading orders.

One reason for asking this question is that, while both the leading and subleading soft-photon theorems have been related to asymptotic symmetries, the nature of these symmetries is subtly different. Namely, the leading-order soft-photon theorem has been associated [20,21] with a group of "large" gauge transformations, those which have finite, angle-dependent limits to null infinity. On the other hand, the symmetries associated with the subleading soft-photon theorem cannot be straightforwardly understood as gauge transformations in their usual form [22] (although some progress has been made on advancing such an interpretation [38]).

So, while dressed states have been constructed even to subleading order [39], only the leading-order dressing is obviously necessary to satisfy constraints imposed by demanding gauge invariance asymptotically [40]. This difference between leading and subleading soft modes will be mirrored in the calculation that follows. The leading-order dressing will turn out to be necessary to alleviate IR divergences, while no such divergences ever appear at subleading order.

To show this, and to quantify the leading and subleading contributions to decoherence, we will use the recent discovery that the leading and subleading soft-photon factors are encoded at the end points of charged-particle world lines [41]. This result allows us to cleanly isolate the quantum information content of both leading and subleading soft photons in our model. What is more, it is not necessary to go to any asymptotic limit to obtain these results. This is important: while many questions about the information content of soft photons are asked in the context of black holes [42] or scattering processes taking place over infinite amounts of time [32,33], we will be able to come to our conclusions even in the context of a somewhat idealized interferometry experiment, in which all processes are confined to a finite space-time region. Thus, we have the possibility of testing for the size of subleading contributions to decoherence, and deciding empirically the question posed above.

Real interferometry experiments, as well as two-slit experiments, are much more complicated than the idealization we introduce. There are multiple other sources of decoherence, including electronic 4-currents (in conducting systems), phonons, two-level systems made from electric dipoles or charges hopping between sites, paramagnetic impurities, and so on; we note that static charges and electric dipoles can interact over long ranges with the electron. One can also consider large neutral objects, but these are polarizable and still interact weakly with long-wavelength photons; however, they typically interact rather strongly with other decoherence sources like phonons. Later in the paper we discuss the experimental prospects in more detail.

B. Summary and structure of the paper

The rest of the paper proceeds as follows. First, in Sec. II we introduce what is by now a standard schematic semiclassical interferometry model. We describe the assumed geometry of the interferometer, and mention the various assumptions and approximations we will use.

Section III introduces the way in which we quantify the which-path information obtained by photons radiated by the superposed charge. As we will show, this can be done rather neatly in terms of the decoherence functional Γ.

In Sec. IV we discuss relevant features of the momentum-space electromagnetic current $j^a(q)$ which appears in the decoherence functional. This allows us to review results from our recent work [41], which showed that boundary terms in the electromagnetic current encode the "soft factors" appearing in both the leading and subleading soft-photon theorems.

We then show in Sec. V that superpositions of the leading soft factor generically cause the decoherence functional Γ to

diverge in the infrared, even for finite-time experiments. We must deal with these infrared divergences properly in order to obtain sensible results for the quantum information content of the photon field, so Sec. V also discusses how we ought to "dress" the time-evolution operator in our semiclassical model in order to render the decoherence functional infrared finite. After adding the appropriate dressing, the leading soft photons cease to obtain any quantum information about the matter particle.

Section VI contains the evaluation of the corrected expression for Γ in our model. We show that subleading soft photons may still contribute to Γ, and we isolate the contribution coming from the difference in the subleading soft current on each branch of the superposition. The subleading contribution to decoherence turns out to be time independent, and to depend only upon the spatial extent of the model interferometer.

Although the inherent IR finiteness of the subleading contribution suggests that subleading dressing is not necessary, ideally the question of whether or not subleading dressing exists should be answered experimentally. Accordingly, Sec. VI C also contains a calculation of decoherence when a simple form of subleading dressing is applied. The results with and without subleading dressing are sufficiently different that we believe it should be in principle possible to detect the presence or absence of this extra dressing in the laboratory.

In any real experiment, however, there will be other processes also causing decoherence: these include coupling of the electron to any gas particles in the experiment, the long-range interaction of the electron with "charge fluctuators" and electronic currents in the apparatus. The first can be understood using scattering theory [43], the second using a "spin bath" theory [44], and the final mechanism using an oscillator bath model for the electronic environment. We discuss these experimental considerations further in Sec. VII.

The paper concludes in Sec. VIII with a discussion of our results, and of some open questions.

Here we use the mostly-negative metric signature, $\eta_{ab} \equiv \mathrm{diag}(1,-1,-1,-1)$, units in which $\hbar = c = \epsilon_0 = 1$, and a bar over a quantity will indicate its complex conjugate.

II. INTERFEROMETER MODEL

Let us begin by introducing the simple model we will use to describe a charged particle traversing an interferometer. We emphasize that although this model is fairly standard in quantum optics [45], it is rather schematic in nature (in Sec. VII we discuss what kind of elaborations may be required for any "real world" treatment of this system). The spatial trajectories taken by the superposed particle are illustrated in Fig. 2. The particle enters the apparatus along the $\hat{x}$ direction with four-velocity $\dot{X}_2^a$; upon reaching the point X_i^a at time $t = 0$, the particle is put into a superposition, in which it is either kicked into the $\hat{y}$ direction to follow the trajectory $X_L^a(s)$, or allowed to proceed in the $\hat{x}$ direction and follow the trajectory $X_R^a(s)$. Here s is the proper time experienced by the particle as it evolves along the trajectories.

As the system then evolves, that branch of the superposition following the trajectory $X_L^a(s)$ (the solid line in Fig. 2) proceeds with the four-velocity $\dot{X}_1^a$ to the point X_L^a, and then with four-velocity $\dot{X}_2^a$ until it reaches the detector **D**. The

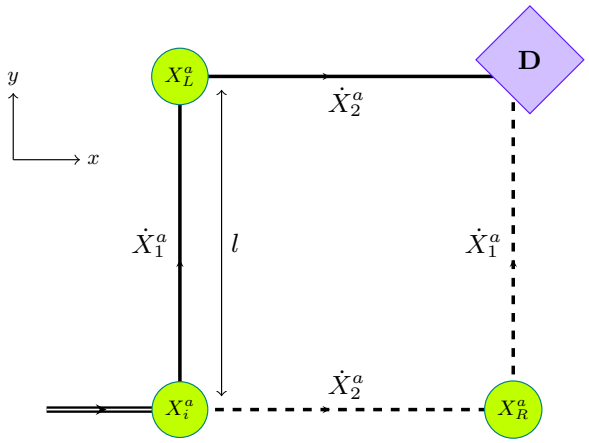

FIG. 2. Top-down view of the two-path geometry traversed by the charged particle.

branch following the trajectory $X_R^a(s)$ (dashed line) proceeds with the four-velocity $\dot{X}_2^a$ to the point X_R^a, and then with four-velocity $\dot{X}_1^a$ to the detector. On both paths, the speed of the particle is taken to be constant at $v \equiv l/\tau$, where l is the length of one side of the interferometer, so that the particle reaches either X_L^a or X_R^a at time $t = \tau$ and reaches the detector at $t = 2\tau$.

Figure 2 is schematic in the sense that, in reality, a *single* path shown going along the left or right trajectory actually represents the set of *all* paths passing through the left arm of an interferometer (this shorthand way of representing entire classes of path originated in Feynman's celebrated description of two-path experiments [1], and can be made more precise than is necessary here [2]). It is assumed in what follows that the experimental setup is "well designed" in the sense that these two classes of electronic path are well separated in space, and that the electronic acceleration when following them is very different for each one of them.

In the computations that follow, we are typically interested in the interaction between the particle and the long-wavelength part of the electromagnetic field. Therefore we assume, following [8,9], that any photons excited during the experiment will have a wavelength which is too large (much larger than the particle's de Broglie wavelength) for them to meaningfully resolve the spread of the particle's wave function. The electromagnetic field in our model then "sees" each trajectory as a single path, and so experiences a simple discrete superposition of two classical electromagnetic currents j_L^a and j_R^a in the interferometer. The assumption that the experimental setup is well designed then means that j_L^a and j_R^a are quite distinct, and so too will be the corresponding photon states.

This leads us to approximate the state of the matter+radiation system as the particle enters the detector **D** using the simple two-path form

$$\frac{1}{\sqrt{2}}[|\psi_L\rangle|L\rangle + |\psi_R\rangle|R\rangle], \tag{2}$$

where $|\psi_{L/R}\rangle$ and $|L/R\rangle$ are the states of the matter particle and the radiation field, respectively, after the particle traverses the L/R arm of the interferometer.

The electromagnetic current of a pointlike particle with charge e, which follows either of the trajectories $X^a_{L/R}(s)$, is

$$j^a_{L/R}(x) = e\int_{s_i}^{s_f} ds\, \dot{X}^a_{L/R}(s)\delta^{(4)}[x - X_{L/R}(s)], \tag{3}$$

where again s is the particle's proper time, and $\dot{X}^a_{L/R}(s) \equiv \frac{d}{ds}X_{L/R}(s)$ its four-velocity. The bounds on this integral are chosen such that the initial and final proper times coincide with the beginning and end of the experiment, $X^0_{L/R}(s_i) = 0$ and $X^0_{L/R}(s_f) = 2\tau$.

Assuming the photon field is in vacuum at the time the experiment starts, under time evolution the electromagnetic environment will be placed into a superposition of coherent photon states, sourced by either the L or R current:

$$|L/R\rangle \equiv \mathcal{T}e^{-i\int d^4x\, j^a_{L/R}(x)\hat{A}_a(x)}|0\rangle. \tag{4}$$

These coherent states are obtained by the action of the interaction-picture time-evolution operator acting on the photon vacuum $|0\rangle$, and here $\mathcal{T}$ denotes time ordering. In writing this expression we have assumed as in (3) that the currents $j^a_{L/R}(x)$ have support only for the duration of the experiment (between s_i and s_f), so we can let the integral $\int d^4x$ run over all values of $t \in (-\infty, +\infty)$.

III. MEASURES OF WHICH-PATH INFORMATION AND DECOHERENCE

Our aim here is to quantify the which-path information gained by the infrared radiation emitted by the charged particle as it proceeds through the interferometer. To do so, we will make use of two standard measures of such information, known as *path distinguishability* and *interferometric visibility* [46–48].

A. Path distinguishability and interferometric visibility

Suppose that some system of interest $\mathcal{S}$ begins in a pure state, and then undergoes two-path interference. Let the state of the system after traversing solely the first and second paths be called $|\mathcal{S}_1\rangle$ and $|\mathcal{S}_2\rangle$, respectively. The state occupied by some which-path measuring device $\mathcal{M}$, also assumed to start in a pure state, after the system traverses the first (second) path, we call $|\mathcal{M}_1\rangle$ ($|\mathcal{M}_2\rangle$). Then after the system follows a balanced superposition of both paths, the combined state of the system and measuring device will be of the form

$$|\Psi\rangle = \frac{1}{\sqrt{2}}[|\mathcal{S}_1\rangle|\mathcal{M}_1\rangle + |\mathcal{S}_2\rangle|\mathcal{M}_2\rangle]. \tag{5}$$

The path distinguishability $\mathcal{D}$ is defined to be the trace distance between the final states $\rho^{\mathcal{M}}_{1/2} \equiv |\mathcal{M}_{1/2}\rangle\langle\mathcal{M}_{1/2}|$ of the measurement apparatus $\mathcal{M}$ on each branch of the superposition:

$$\mathcal{D} \equiv \tfrac{1}{2}\mathrm{Tr}\big|\rho^{\mathcal{M}}_1 - \rho^{\mathcal{M}}_2\big| = \sqrt{1 - |\langle\mathcal{M}_2|\mathcal{M}_1\rangle|^2}. \tag{6}$$

This path distinguishability yields an upper bound to the likelihood $\mathcal{L}$ of successfully discriminating between the two paths taken by the system $\mathcal{S}$ by observing only the degrees of freedom of the measurement device $\mathcal{M}$, as $\mathcal{L} \leqslant \frac{1}{2}(1 + \mathcal{D})$ [48], making it the natural measure of how much which-path information is contained in $\mathcal{M}$.

The interferometric visibility $\mathcal{V}$, on the other hand, quantifies how easy it is to observe the coherence of the system $\mathcal{S}$. $\mathcal{V}$ is typically defined in the context of double-slit interferometry as

$$\mathcal{V} \equiv \frac{I_{\max} - I_{\min}}{I_{\max} + I_{\min}}, \tag{7}$$

where $I_{\max}$ and $I_{\min}$ are the maximum and minimum intensities of the interference fringes on a screen. More generally it obeys the upper bound

$$\mathcal{V} \leqslant |\langle\mathcal{M}_2|\mathcal{M}_1\rangle|, \tag{8}$$

though its precise form depends upon the specifics of the interferometer (see, for example, [49] for an explicit calculation of $\mathcal{V}$ in a double-slit interferometer).

Equations (6) and (8) lead immediately to the well-known "duality relation" between distinguishability and visibility,

$$\mathcal{D}^2 + \mathcal{V}^2 \leqslant 1. \tag{9}$$

This relation expresses the fact that the acquisition of quantum information is generally destructive; the more which-path information is obtained by $\mathcal{M}$, the less coherent $\mathcal{S}$ will appear.

B. Electromagnetic field as a measuring device

Let us now return to the charged particle introduced in the previous section. Clearly the combined state in Eq. (2) has the same form as (5), with the role of $\mathcal{S}$ played by the moving charge, and $\mathcal{M}$ played by the photon field. Quantifying the amount of which-path information carried away via photon emission, and the resulting loss of interferometric visibility, then follows immediately. The which-path information gained by the photons is

$$\mathcal{D} = \sqrt{1 - |\langle R|L\rangle|^2}, \tag{10}$$

and the interferometric visibility in an experiment of the form we consider is bounded from above according to

$$\mathcal{V} \leqslant |\langle R|L\rangle|. \tag{11}$$

In our toy-model interferometry setup the quantity governing both the visibility $\mathcal{V}$ and the distinguishability $\mathcal{D}$, and therefore how much which-path information is obtained by the electromagnetic field, is then the modulus of the inner product between the photon coherent states, which we write in the form

$$|\langle R|L\rangle| \equiv e^{-\Gamma}; \quad \Gamma \in \mathbb{R}, \quad \Gamma \geqslant 0. \tag{12}$$

The quantity Γ appearing is just the well-known *decoherence functional* [5,7,50,51], so called because it is a functional of the currents along the entire L and R paths, i.e., $\Gamma \equiv \Gamma[j_L, j_R]$. It thus depends on everything that happens to the charge on each of these paths, and neatly encodes the process of emission of which-path information into the electromagnetic environment.

In the case that the decoherence is very small, and we do expect the contribution to decoherence coming from radiation of infrared photons to be small in laboratory settings, we can

approximate $|\langle R|L\rangle| \approx 1-\Gamma$. Then we have

$$\mathcal{D} \approx \Gamma; \qquad \mathcal{V} \lesssim 1-\Gamma. \tag{13}$$

The decoherence functional and the path distinguishability are equivalent in the context of our model interferometry experiment as measures of how much which-path information is obtained by the radiated photons, and Γ also directly quantifies the loss of visibility due solely to photon emission. Because Γ so cleanly captures the tradeoff between $\mathcal{D}$ and $\mathcal{V}$, we will work solely with Γ in what follows.

IV. FORM OF ELECTROMAGNETIC CURRENTS AND DECOHERENCE FUNCTIONAL

The electromagnetic decoherence functional was first derived long ago [51,52], and has been discussed more recently, e.g., by Ford [8], and by Breuer and Petruccione [9]. At zero temperature it takes the form

$$\Gamma[j_L, j_R] = \frac{1}{2}\int \frac{d^3q}{(2\pi)^3 2\omega}\, P_{ab}\, \delta j^a(q)\delta j^b(-q), \tag{14}$$

where $\delta j^a \equiv j^a_L - j^a_R$ is the difference in electromagnetic currents along the two superposed paths, $q^a \equiv \omega(1,\hat{n})$, with $\hat{n}$ an angular unit vector, is a null four-momentum, and $\int \frac{d^3q}{(2\pi)^3} \equiv \oint \frac{dS^2(\hat{n})}{(2\pi)^2}\int_0^\infty \frac{d\omega}{2\pi}\omega^2$. Finally, the transverse projector P_{ab} can be written in terms of the momentum q^a as $P_{jk} \equiv \delta_{jk} - \frac{q_j q_k}{\omega^2}$, with $P_{0a} = 0$.

Note that Γ as written is a functional of currents which may have support for times $t \in (-\infty, +\infty)$. However, we have restricted to finite-time dynamics here by restricting the range of the proper time integrals in (3).

Let us now further discuss the matter currents we will insert into the decoherence functional (14); we will wish to understand in particular the various contributions to the decoherence functional, which is central to any analysis of decoherence, for any system, coming from the end points of the particle's paths through the interferometer.

What appears in the decoherence functional is actually the Fourier transform of the current $j^a(q) \equiv \int d^4x\, e^{iq\cdot x} j^a(x)$, which using (3) is

$$j^a(q) \;=\; e\int ds\, \dot{X}^a(s)\, e^{iq\cdot X(s)}, \tag{15}$$

which we rewrite as

$$j^a(q) \;=\; e\int ds\, \dot{X}^a \left(\frac{1}{iq\cdot\dot{X}}\right)\frac{d}{ds}e^{iq\cdot X}, \tag{16}$$

so that integrating by parts in s gives

$$\begin{aligned} j^a(q) = &-ie\int ds\, \frac{d}{ds}\left(e^{iq\cdot X}\,\frac{\dot{X}^a}{q\cdot\dot{X}}\right) \\ &+ ie\int ds\, e^{iq\cdot X}\,\frac{d}{ds}\left(\frac{\dot{X}^a}{q\cdot\dot{X}}\right). \end{aligned} \tag{17}$$

Discarding the boundary term appearing here [41,53,54] ensures that the current is conserved, $q_a j^a(q) = 0$, leaving us with the following corrected expression for the particle current in momentum space:

$$j^a(q) = ie\int ds\, e^{iq\cdot X}\,\frac{d}{ds}\left(\frac{\dot{X}^a}{q\cdot\dot{X}}\right). \tag{18}$$

Notice that the form (18) of the matter current has the property that the current vanishes when the particle is not accelerating ($\ddot{X}^a = 0$).

Plugging the current into the decoherence functional (14), we note immediately the important fact that *there is no decoherence without acceleration* because the decoherence in this system arises purely as a result of of radiative coupling to the photon field.

A. Soft electromagnetic currents

Previously we showed [41] that the electromagnetic current of a point particle (18) is the sum of two terms, each of which which are entirely localized on the boundary (i.e., the end points) of the world line the particle traces out in space-time. These boundary terms turn out to be those parts of the current which dominate at low frequencies.

In particular we showed that expanding (18) in powers of q we get

$$ij^a(-q) = e\big[\Delta\big[\mathcal{S}^a_{(0)}(q, m\dot{X})\big] + \Delta\big[\mathcal{S}^a_{(1)}(q, X, m\dot{X})\big]\big] + O(q), \tag{19}$$

where, if the proper time integral in (18) runs from s_i to s_f, then the $\Delta[\dots]$ in this expression has the meaning

$$\Delta[f(s)] \equiv f(s_f) - f(s_i) = \int_{s_i}^{s_f} \partial_s f(s), \tag{20}$$

showing that these contributions live on the end points of the particle world line, at s_i and s_f, and we have defined the leading and subleading electromagnetic "soft factors"

$$\mathcal{S}^a_{(0)}(q,p) \equiv \frac{p^a}{q\cdot p}, \quad \mathcal{S}^a_{(1)}(q,x,p) \equiv i\frac{q_b J^{ba}}{q\cdot p}. \tag{21}$$

Here, $J^{ab} \equiv 2p^{[a}x^{b]}$ is the angular momentum tensor. Reference [41] further showed that these boundary terms explain the factorization of the leading and subleading soft-photon theorems at tree level.

We emphasize that these boundary terms on the world line are *not* necessarily located at asymptotic coordinate times $t \to \pm\infty$. They exist and take the form (19) for any choice of bounds on the proper time integral in (18).

From Eq. (19) it is then clear that we can always split the point particle current into three pieces, viz.,

$$j^a(q) \equiv j^a_{\rm div}(q) + j^a_{\rm sub}(q) + j^a_{\rm hard}(q), \tag{22}$$

with

$$\begin{aligned} j^a_{\rm div}(q) &\equiv ie\Delta\left[\frac{\dot{X}^a}{q\cdot\dot{X}}\right], \\ j^a_{\rm sub}(q) &\equiv e\Delta\left[\frac{q_b[X^a\dot{X}^b - \dot{X}^a X^b]}{q\cdot\dot{X}}\right], \\ j^a_{\rm hard}(q) &\equiv j^a(q) - j^a_{\rm div}(q) - j^a_{\rm sub}(q). \end{aligned} \tag{23}$$

We interpret the currents $j^a_{\rm div}$, $j^a_{\rm sub}$, and $j^a_{\rm hard}$ as the sources of leading soft radiation, subleading soft radiation, and hard

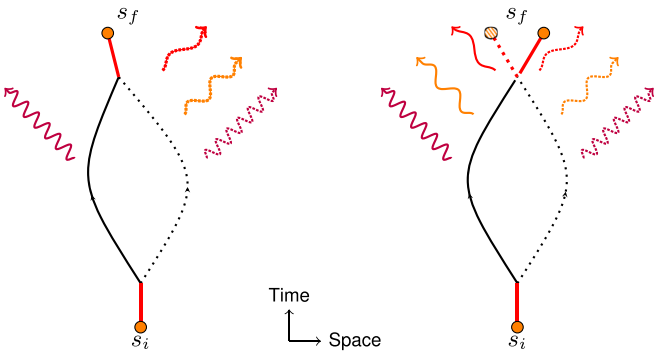

FIG. 3. Left: two charged-particle trajectories which source different hard radiation, but the same soft radiation. Right: two trajectories which source different hard and soft radiation, due to differences in the soft currents $j^a_{\rm div}$ and $j^a_{\rm sub}$ at the world-line boundary. The hard radiation is shown as the shortest wavelength emission, in purple; the leading soft radiation shown as the longest wavelength emission, in red; and the subleading soft radiation in orange.

radiation, respectively. In this work, we then *define* "leading soft radiation" as radiation which is sourced by $j^a_{\rm div}$, "subleading soft radiation" as radiation which is sourced by $j^a_{\rm sub}$, and "hard radiation" as radiation which is sourced by the remaining term $j^a_{\rm hard}$. This interpretation is illustrated in Fig. 3.

We note immediately that the leading soft current $j^a_{\rm div}$ is *infrared divergent*, as it goes like $1/\omega$ and blows up as $\omega \to 0$. The subleading soft current $j^a_{\rm sub}$ is, however, $O(1)$ and perfectly infrared finite, and the hard current $j^a_{\rm hard}$ is $O(\omega)$ and vanishes completely in the soft $\omega \to 0$ limit. Additionally, we note that each of these currents is individually conserved, i.e.,

$$q_a j^a_{\rm div}(q) = q_a j^a_{\rm sub}(q) = q_a j^a_{\rm hard}(q) = 0. \tag{24}$$

The identification of these soft currents will allow us to rather directly assess the contribution to the decoherence functional (14) from leading and subleading soft-photon modes. In particular, we will expand the decoherence functional (14) in terms of the splitting (22) to get

$$\Gamma = \frac{e^2}{2}\int \frac{d^3q}{(2\pi)^3 2\omega}\, P_{ab}\big[\delta j^a_{\rm div}(q) + \delta j^a_{\rm sub}(q) + \delta j^a_{\rm hard}(q)\big] \times \big[\delta j^b_{\rm div}(-q) + \delta j^b_{\rm sub}(-q) + \delta j^b_{\rm hard}(-q)\big], \tag{25}$$

displaying clearly the contributions from the leading and subleading soft currents to Γ.

We will see later on that this expression for Γ is unphysical since it contains divergent terms that in the end make no contribution. The true physical form for Γ will be given in Eq. (37) below.

B. Decoherence functional for interferometer

The general form of a decoherence functional Γ is independent of the geometry of the system, but we will now need the specific form for our two-path system. To obtain this, we first write the electromagnetic currents along the left and right trajectories as

$$j^a_L(q) = ie\int ds\, e^{iq\cdot X_L(s)}\partial_s\left[\frac{\dot X^a_L(s)}{q\cdot \dot X_L(s)}\right],$$
$$j^a_R(q) = ie\int ds\, e^{iq\cdot X_R(s)}\partial_s\left[\frac{\dot X^a_R(s)}{q\cdot \dot X_R(s)}\right]. \tag{26}$$

The difference between the two currents on the superposed paths,

$$\delta j^a(q) \equiv j^a_L(q) - j^a_R(q), \tag{27}$$

can then be approximated in the geometry illustrated in Fig. 2 as

$$\delta j^a(q) = ie\,[e^{iq\cdot X_i} - e^{iq\cdot X_L} - e^{iq\cdot X_R}]\left[\frac{\dot X^a_1}{q\cdot \dot X_1} - \frac{\dot X^a_2}{q\cdot \dot X_2}\right]. \tag{28}$$

Notice that the current difference consists of terms associated with the points X^a_i, X^a_L, and X^a_R. These are the space-time events at which the particle accelerates and thence radiates photons.

Expressions like (25) and (28) can only be used once the trajectories for the electron are specified. This can only be done in detail for a specific experimental setup (for which see Sec. VII). In what follows we will simply assume the following: (i) that the particle travels nonrelativistically, by which we mean that its velocity v satisfies

$$v \equiv \frac{l}{\tau} \ll 1 \tag{29}$$

in units with $c = 1$, then we can assume that the spatial parts of the phases appearing in (28) can be neglected to leading order. This is just the well-known dipole approximation [55]; we are assuming, as noted in the Introduction, that the radiation emitted during the experiment will have a wavelength that is long compared to the spatial extent of the interferometer, and so cannot resolve the spatial separation of the points at which the particle radiates. We will also assume (ii) that the spatial extent of the "scattering" regions $X^a_{\{i,L,R\}}$ inside of which the particle experiences acceleration can be characterized by a length scale $l_0 \equiv 1/\Omega$, where Ω effectively acts as a UV frequency cutoff for the scattering. It follows that l_0 is then the shortest length scale relevant to our analysis. An ultraviolet cutoff Ω of this sort also emerges naturally if one smears out the superposed trajectories we are considering, allowing the currents to have support along world tubes of finite width $\sim 1/\Omega$, rather than on perfectly localized one-dimensional world lines [9].

Note that the timescale τ over which the experiment occurs is then long, in the sense that $\Omega\tau \gg 1$, because $v \ll 1$. To put it another way, the timescale τ is much greater than the time it takes light to cross the scattering regions, of size $1/\Omega$.

With these assumptions in place, the current difference can be further simplified to

$$\delta j^a(q) \approx ie(1 - 2e^{i\omega\tau})\left[\frac{\dot X^a_1}{q\cdot \dot X_1} - \frac{\dot X^a_2}{q\cdot \dot X_2}\right]. \tag{30}$$

Plugging this current difference into the decoherence functional gives

$$\Gamma \approx \frac{e^2}{4(2\pi)^3}\int_\lambda^\Omega \frac{d\omega}{\omega}\,(5-4\,\cos\omega\tau)\oint dS^2(\hat{n})\,\omega^2 \times\left[2\frac{\dot{X}_1\cdot\dot{X}_2}{(q\cdot\dot{X}_1)(q\cdot\dot{X}_2)}-\frac{1}{(q\cdot\dot{X}_1)^2}-\frac{1}{(q\cdot\dot{X}_2)^2}\right]. \tag{31}$$

The spherical integral here is independent of ω since the term in square brackets goes like $\frac{1}{\omega^2}$ and this gets multiplied by the factor ω^2 from the integration measure.

The result (31) for Γ incorporates all the soft contributions; what we will now show is that the contribution from the leading divergent contributions is actually zero.

V. LEADING-ORDER SOFT PHOTONS

In order for the integral (31) to be well defined, we have also been forced to introduce an infrared cutoff λ. The integrand of (31) diverges like $1/\omega$ as $\omega\to 0$, so the frequency integral goes to infinity like $-\ln\lambda$ as we take the infrared cutoff $\lambda\to 0$. Taken naïvely, this leads one to predict an infinite amount of decoherence since $\Gamma\to\infty$ in the IR limit; this is clearly unphysical.

In earlier discussion of IR divergences, noted in the Introduction, it was necessary to introduce complicated devices (e.g., measuring systems designed to observe IR photons) to deal with these divergences, and show how they were either canceled or otherwise eliminated. However, in what follows we will show how our understanding of soft currents allows these divergences to be handled in a fairly straightforward way, which simply reduces their contribution to Γ to zero.

A. Infrared divergences

In Sec. IV, we saw that the divergence in question is due to a superposition of the leading contribution to the soft current; $\delta j^a_{\rm div}$ is not zero in this example. Begin by splitting the current (30) into its relevant soft [$O(\omega^{-1})$ and $O(1)$] and hard [$O(\omega)$] pieces. In this model we have $\delta j^a \equiv \delta j^a_{\rm div}+\delta j^a_{\rm sub}+\delta j^a_{\rm hard}$, with

$$\begin{aligned}\delta j^a_{\rm div}(q) &\approx -ie\left[\frac{\dot{X}_1^a}{q\cdot\dot{X}_1}-\frac{\dot{X}_2^a}{q\cdot\dot{X}_2}\right],\\ \delta j^a_{\rm sub}(q) &\approx 2e\omega\tau\left[\frac{\dot{X}_1^a}{q\cdot\dot{X}_1}-\frac{\dot{X}_2^a}{q\cdot\dot{X}_2}\right],\\ \delta j^a_{\rm hard}(q) &\approx 2ie(1-e^{i\omega\tau}+i\omega\tau)\left[\frac{\dot{X}_1^a}{q\cdot\dot{X}_1}-\frac{\dot{X}_2^a}{q\cdot\dot{X}_2}\right]\end{aligned} \tag{32}$$

in the dipole approximation.

From the general form of the decoherence functional (25), we see that Γ contains a term involving only the leading soft current $j^a_{\rm div}$:

$$\Gamma \supset \frac{1}{2}\int\frac{d^3q}{(2\pi)^3 2\omega}\,P_{ab}\,\delta j^a_{\rm div}(q)\delta j^b_{\rm div}(-q) = \frac{e^2}{4(2\pi)^3}\int_\lambda^\Omega\frac{d\omega}{\omega}\oint dS^2(\hat{n})\,\omega^2\left[2\frac{\dot{X}_1\cdot\dot{X}_2}{(q\cdot\dot{X}_1)(q\cdot\dot{X}_2)}-\frac{1}{(q\cdot\dot{X}_1)^2}-\frac{1}{(q\cdot\dot{X}_2)^2}\right]. \tag{33}$$

It is this term that causes the infrared divergence when taking $\lambda\to 0$, seen here as the logarithmically divergent integral $\int_\lambda^\Omega\frac{d\omega}{\omega}$. The infrared divergence is caused by a superposition of the leading soft current, i.e., $\Gamma\to\infty$ because $\delta j^a_{\rm div}\neq 0$. The resulting infinite amount of decoherence should thus be understood as coming from information loss into leading soft-photon modes.

B. Infrared dressing

If this result turned out to be the end of the story, then the leading-order soft photons would always make a perfect which-path measurement of the charged particle in any experiment of the sort shown in Fig. 2. This is obviously wrong: if it were the case, we would have $\Gamma\to\infty$ for *any* choice of experimental parameters (e, l, τ), and from Eqs. (11) and (12) we see that there would *never* be any observable interference once the particle reaches the detector! Because quantum interference is observed in Nature, we must reject this result.

This conclusion is not new, and indeed has informed all investigations of IR divergences in QED since Bloch and Nordsieck [10]. That one needs to properly handle these divergences is also obvious in the eikonal formulation of QED [23,24] and was a motivating factor in the coherent state formulation of QED in terms of dressed states [26–32]. In the coherent state formulation, the IR divergences are eliminated by dressing the electron, so that soft photons appear already in the time evolution operator.

It turns out to be incredibly simple to effect IR dressing in our treatment. We show in Appendix A that the net effect of applying a "minimal" implementation of the dressed formalism, which we define in that Appendix, is that we can simply set the divergent soft current $j^a_{\rm div}$ to zero everywhere in our calculations: the physical result of IR dressing can then be interpreted as the total decoupling of $j^a_{\rm div}$ from the Maxwell field. After incorporating the dressing, when studying the electromagnetic radiation caused by the charged particle moving through our model interferometer, what we do is define *dressed coherent states* in the same way as we defined the coherent radiation states in Eq. (4), but now we explicitly subtract out the divergent current $j^a_{\rm div}$, i.e., we write

$$||L/R\rangle\rangle \equiv \mathcal{T}e^{-i\int d^4x\,[j^a_{L/R}-j^a_{L/R,\rm div}](x)\hat{A}_a(x)}|0\rangle. \tag{34}$$

We can then define a *dressed decoherence functional* in the same way we defined Γ in the "undressed" case, but using the dressed coherent states instead:

$$|\langle\langle R|L\rangle\rangle| \equiv e^{-\Gamma_{\rm dressed}}. \tag{35}$$

The dressed decoherence functional $\Gamma_{\rm dressed}$ can be obtained from the undressed decoherence functional (25) by simply

setting the divergent current $j^a_{\rm div}$ to zero, giving

$$\Gamma_{\rm dressed} = \frac{e^2}{2}\int \frac{d^3q}{(2\pi)^3 2\omega}\, P_{ab}\big[\delta j^a_{\rm sub}(q) + \delta j^a_{\rm hard}(q)\big] \times \big[\delta j^b_{\rm sub}(-q) + \delta j^b_{\rm hard}(-q)\big]. \tag{36}$$

The expression (36) makes it clear that in the dressed formalism, the leading soft current no longer plays a role in decoherence of the matter state. Because infrared divergences necessitate this dressing, we conclude that leading soft photons do not cause decoherence, and therefore do not carry any quantum information about the matter.

VI. SUBLEADING SOFT PHOTONS

After having "dressed away" the leading soft-photon contributions to decoherence, we can now begin our study of the remaining subleading contributions. We will do this by once more evaluating the decoherence functional, but this time using the dressed expression (36).

A. Dressed decoherence functional

We begin by inserting the subleading and hard parts of the current difference from (32) into (36) to give

$$\Gamma_{\rm dressed} \approx \frac{2e^2}{(2\pi)^3}\int_0^\Omega \frac{d\omega}{\omega}\,(1-\cos\omega\tau)\oint dS^2(\hat{n})\,\omega^2 \times\left[2\frac{\dot{X}_1\cdot\dot{X}_2}{(q\cdot\dot{X}_1)(q\cdot\dot{X}_2)} - \frac{1}{(q\cdot\dot{X}_1)^2} - \frac{1}{(q\cdot\dot{X}_2)^2}\right]. \tag{37}$$

This expression incorporates both the subleading current difference $\delta j^a_{\rm sub}(q)$, and the hard current difference $\delta j^a_{\rm hard}(q)$, and cross terms between them. We stress that since the contribution from the divergent leading photon terms to Γ is zero, Eq. (37) should be regarded as the correct expression for the decoherence functional.

We see that after incorporating the infrared dressing, the integrand of the frequency integral now goes to zero as $\omega \to 0$, killing off the divergence we found before, and rendering the integral finite so that we can evaluate it properly, even with the infrared cutoff λ now taken to zero. The dressing is working as intended.

To arrive at (37), we have again assumed that the particle travels through the interferometer nonrelativistically, $v \ll 1$; as discussed earlier, this allowed us to invoke the dipole approximation, in which we ignored spatial parts of the phases appearing in the decoherence functional. When evaluating $\Gamma_{\rm dressed}$ we can again assume that $\Omega\tau \gg 1$, i.e., that the timescale τ of the experiment τ is such that $\tau \gg 1/\Omega$.

We evaluate the expression (37) using these approximations in Appendix B 1, with the result that the result for decoherence from the leading contributions is

$$\Gamma_{\rm dressed} \approx \frac{4e^2v^2}{3\pi^2}\ln\Omega\tau, \tag{38}$$

which agrees with previous calculations of electromagnetic decoherence [9,56].

As expected, this decoherence is coming from dipolar electromagnetic radiation; we can write $\Gamma_{\rm dressed} \propto (\partial_t e\delta x)^2$, where $e\delta x$ is the difference in electric dipole moments between the L and R branches.

B. Purely subleading contribution

In addition to computing the full amount of photon decoherence in our model, let us now take a short detour to compute the decoherence coming only from the subleading terms in our dressed expression (37) for $\Gamma_{\rm dressed}$.

In the general form (36) of the dressed decoherence functional, we see that the purely subleading term $P_{ab}\delta j^a_{\rm sub}\delta j^b_{\rm sub}$, the cross terms $P_{ab}\delta j^a_{\rm sub}\delta j^b_{\rm hard}$, and the purely hard part $P_{ab}\delta j^a_{\rm hard}\delta j^b_{\rm hard}$ are all of different orders in $\omega\tau$, and so can be classified according to this order. The first purely subleading term gives decoherence caused purely by superpositions of the subleading soft current. Writing this contribution as $\Gamma_{\rm sub}$, we then have

$$\begin{aligned}\Gamma_{\rm sub} &\equiv \frac{1}{2}\int \frac{d^3q}{(2\pi)^3 2\omega}\, P_{ab}\,\delta j^a_{\rm sub}(q)\delta j^b_{\rm sub}(-q)\\ &= \frac{e^2}{(2\pi)^3}\int_0^\Omega d\omega\,\omega\tau^2\oint dS^2(\hat{n})\,\omega^2\\ &\quad\times\left[2\frac{\dot{X}_1\cdot\dot{X}_2}{(q\cdot\dot{X}_1)(q\cdot\dot{X}_2)} - \frac{1}{(q\cdot\dot{X}_1)^2} - \frac{1}{(q\cdot\dot{X}_2)^2}\right],\end{aligned} \tag{39}$$

where we have used the expression for $\delta j^a_{\rm sub}$ found in Eq. (32), and where we see that this result is nothing but the lowest-order term in the expansion of the integrand of (37) in powers of $\omega\tau$.

The quantity $\Gamma_{\rm sub}$ has an intuitive interpretation. Imagine allowing the electromagnetic field to couple *only to the subleading soft current* $j^a_{\rm sub}$ during our hypothetical interferometry experiment. The resulting states of the electromagnetic radiation sourced by the subleading current on the L/R branches would then be

$$||l/r\rangle\rangle \equiv \mathcal{T}e^{-i\int d^4x\, j^a_{L/R,\rm sub}(x)\hat{A}_a(x)}|0\rangle, \tag{40}$$

and $\Gamma_{\rm sub}$ would encode the modulus of the inner product between these two states as

$$|\langle\langle r|l\rangle\rangle| \equiv e^{-\Gamma_{\rm sub}}. \tag{41}$$

$\Gamma_{\rm sub}$ is then a decoherence functional in its own right, and is the natural measure of the decoherence caused by the electromagnetic field's direct response to a superposition of subleading soft currents.

We evaluate the subleading contribution (39) in Appendix B 2. The result is that the purely subleading contribution to $\Gamma_{\rm dressed}$ is

$$\Gamma_{\rm sub} \approx \frac{e^2}{3\pi^2}\Omega^2v^2\tau^2. \tag{42}$$

Because $v \equiv l/\tau$, this expression is equivalent to

$$\Gamma_{\rm sub} \approx \frac{e^2}{3\pi^2}\Omega^2l^2 \equiv \frac{e^2}{3\pi^2}\left(\frac{l}{l_0}\right)^2, \tag{43}$$

where we have used the fundamental length scale $l_0 \equiv 1/\Omega$ defined by our ultraviolet cutoff.

The result (43) is then that the purely subleading contribution to $\Gamma_{\rm dressed}$ has a remarkable form: it only depends upon the

strength of the coupling e of the particle to the electromagnetic field, and on the size of the interferometer l, measured in units of l_0, the size of a "pixel" in the implicit coarse graining of space-time implied by our use of an ultraviolet cutoff. Unlike the expression (38) for the total amount of decoherence, this purely subleading soft contribution does not depend directly upon the particle's velocity v or on the time τ taken to carry out the experiment.

C. Subleading dressing

Unlike the leading-order contribution, the subleading contribution to decoherence is infrared finite. The subleading part, however, does arise via the same physical mechanism as the leading part, from a boundary term in the electric current. Should we then apply infrared dressing at the subleading order [39], just as we did at leading order?

There are no obviously unphysical divergences which arise in our calculation at subleading order, so it does not seem that the consistency of the theory itself demands further dressing. Instead, we should ask whether the question might be able to be settled experimentally.

To that end, let us consider a specific form of the potential subleading dressing. We will assume that, if such dressing were to exist, we may apply it semiclassically by simply setting $j^a_{\rm sub}$ to zero everywhere, exactly analogous to the way in which applied the leading-order dressing. Setting both the leading and subleading soft currents to zero leaves only the hard current $j^a_{\rm hard}$ to contribute to the decoherence functional:

$$\Gamma_{\rm hard} \equiv \frac{1}{2}\int \frac{d^3q}{(2\pi)^3 2\omega}\, P_{ab}\,\delta j^a_{\rm hard}(q)\delta j^b_{\rm hard}(-q) = \frac{e^2}{(2\pi)^3}\int_0^\Omega \frac{d\omega}{\omega}\,(2-2\,\cos\omega\tau + i\omega\tau e^{i\omega\tau} - i\omega\tau e^{-i\omega\tau} + \omega^2\tau^2)$$
$$\times \oint dS^2(\hat{n})\,\omega^2\left[2\frac{\dot{X}_1\cdot\dot{X}_2}{(q\cdot\dot{X}_1)(q\cdot\dot{X}_2)} - \frac{1}{(q\cdot\dot{X}_1)^2} - \frac{1}{(q\cdot\dot{X}_2)^2}\right], \tag{44}$$

where the expression for $\delta j^a_{\rm hard}$ comes from Eq. (32).

We evaluate this expression in Appendix B 3, with the result

$$\Gamma_{\rm hard} \approx \frac{e^2}{3\pi^2}v^2\left[2\,\ln\Omega\tau + \frac{1}{2}\Omega^2\tau^2\right], \tag{45}$$

in the limit $\Omega\tau \gg 1$. Comparing this result to the prediction (38) after only the leading dressing had been applied, we see that applying the subleading dressing increases the predicted amount of decoherence substantially. The decoherence now grows quadratically with $\Omega\tau$ rather than logarithmically, and by Eqs. (11) and (12), this implies that the visibility of any interference effects will decrease accordingly.

We are now faced with an interesting choice. On the one hand one can argue that the prediction (38) is consistent with well-known prior work, and that the addition of subleading dressing seems to increase the predicted decoherence drastically over that well-known result. Then, a conservative point of view would say that subleading dressing is not necessary. However, one can also argue that, in the absence of strong theoretical arguments, the question of whether subleading dressing exists should be settled by an appropriate experiment, here, an interferometric experiment. The marked difference between the predicted decoherence rates with and without subleading dressing suggests that this such an experiment would not be unfeasible. We stress that such an experiment must take great care to respect the boundary conditions we have imposed upon the particle trajectories in our toy model, if it is to be sensitive to the infrared effects we have studied here. The importance of this question is such that we need to go beyond toy models and discuss what a real experiment might look like; this we now do.

VII. EXPERIMENTAL IMPLICATIONS

Any realistic experiment that tries to observe the presence or absence of subleading soft dressing will be fraught with "real world" complexities. This is partly because the purely photonic decoherence depends very much on the sample geometry. But even more important is that in any real experiment there are lots of other decoherence sources. A proper discussion of these would inevitably occupy many papers.

Accordingly, in what follows we try to satisfy a more limited goal, viz., (i) estimating the soft-photon decoherence effects arise in two model experiments, and (ii) estimating the size of the other decoherence effects which will also appear. To focus the discussion we consider two specific experiments, viz., a two-slit diffraction experiment with electrons, and an interferometric experiment with massive particles. We do not do any really detailed calculations, but rather indicate what will be involved in such calculations, and what kind of answers one expects.

A. Two-slit system

The two-slit experiment for electrons is of course well known [1]; however, the real physical processes taking place during the passage of an object through the slit regions are actually quite complex. To focus the discussion, consider the idealized setup shown in Fig. 4.

The object $\mathcal{S}$ passing through this idealized system may be an electron, which typically will have a long wavelength λ compared to either the slit width b_o or the thickness a_o of the slit plate $\mathcal{M}_2$, i.e., $\lambda \gg a_o, b_o$. Alternatively, we can consider some larger object, such a a large molecule, or, e.g., an insulating nanoparticle made of SiO_2, or a conducting metallic nanoparticle; in this case one may have $\lambda \ll a_o, b_o$. Experiments are in principle possible in both limits, but the physics is quite different in the two cases. In a real two-slit system of this kind surface irregularities may be important in the short-wavelength limit (compare Fig. 5). The irregular shape of the surface can be modeled in various ways; typically one uses a disordered scattering potential and averages over the disorder. Note that this is not a decoherence mechanism,

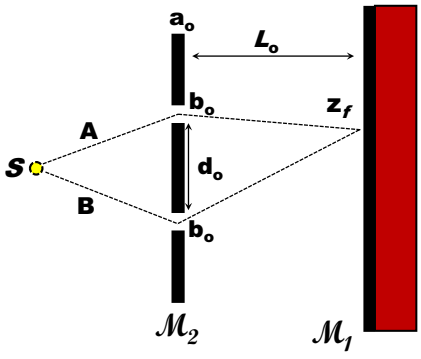

FIG. 4. An idealized view of a two-slit interference system. An object $\mathcal{S}$ can follow either path A or path B through the slit system $\mathcal{M}_2$ to a final coordinate z_f on the screen $\mathcal{M}_1$. the plate $\mathcal{M}_2$ has thickness a_o; each slit has width b_o, with distance d_o between slits, and distance L_o from $\mathcal{M}_2$ to $\mathcal{M}_1$.

however, it will cause unwanted overlap of the L and R electron states. We will therefore treat it as an unwanted feature of the experiment, and assume that a well-designed experiment will have eliminated such irregularities. In the long-wavelength limit $\lambda \gg a_o, b_o$, each slit effectively reradiates the electron states, and one can analyze this using the usual treatment [8]. If we are to find the experimental decoherence rate for this system, we need to understand the role of mechanisms other than the long-wavelength photon decoherence mechanism we are looking for. These include the following:

(i) Discrete surface degrees of freedom associated with unpaired surface electrons ("dangling bonds"), or other dynamic impurity or defect modes which may be on the surface or in this bulk. These degrees of freedom are usually modeled as a "two-level system" environment [44,57]; on the macroscopic scale a large set of such fluctuating two-level systems tend to show up experimentally as fluctuating "patch potentials" [58].

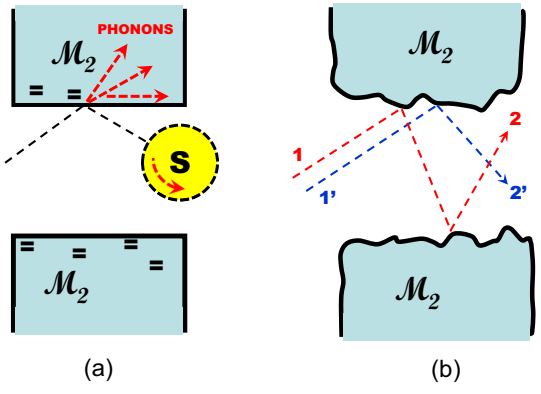

FIG. 5. In (a) we show some of the scattering processes occurring when an extended body $\mathcal{S}$ passes through an idealized slit. Collision between $\mathcal{S}$ and the slit can create bulk or surface phonons, which can, e.g., set $\mathcal{S}$ into rotation. It can also interact with two-level systems in $\mathcal{M}_2$. In (b) we show paths $1 \to 2$ and $1' \to 2'$ for two incoming systems with identical momentum and energy, but displaced from each other. We will reject any experimental design in which such processes are important.

The effect of these defects is to (a) electrostatically perturb the paths of the electrons, and (b) cause decoherence in their dynamics, which can be modeled using a "spin bath" model [44] for the coupling to this environment. At low temperatures this is often the main source of environmental decoherence in the motion of $\mathcal{S}$.

(ii) Both surface and bulk phonons in the slit system can interact with $\mathcal{S}$ as it passes through the slit, with energy and momentum exchange between $\mathcal{S}$ and the slit system $\mathcal{M}_2$. If the slit system is conducting, then the electron motion can also excite gapless surface electronic excitations. The effect of interaction with these modes causes more environmental decoherence: these effects can be modeled using an "oscillator bath" model [59] for this environment, and this oscillator bath decoherence will dominate at higher energies or higher T over the spin bath decoherence.

(iii) At finite temperatures, $\mathcal{S}$ will interact with a thermal bath of photons while traversing the system. In an evacuated two-slit system, the photon bath temperature will be determined by the temperature of the walls of the system, and of the slit and screen system.

The way in which these different effects can alter the dynamics of $\mathcal{S}$ is shown schematically in Fig. 5. If we ignore surface shape irregularities, then we have the situation shown schematically in Fig. 5(a), in which both surface and bulk phonons can be emitted or absorbed by $\mathcal{S}$, with a scattering matrix element $\Gamma(\epsilon, \epsilon'; \mathbf{k}, \mathbf{k}')$ between energy and momentum states $(\epsilon, \mathbf{k})$ and $(\epsilon', \mathbf{k}')$ that needs to be determined from microscopic theory (taking into account that one may emit single- or multiple-phonon excitations).

Note that $\mathcal{S}$, if it is an extended object like a molecule or particle, will have many internal degrees of freedom as well; these may be rotational, vibrational, or discrete (as in, e.g., spin or vibron modes). Thus, as $\mathcal{S}$ scatters off $\mathcal{M}_2$, any of these modes can be excited, and this will also be incorporated in a detailed calculation of the scattering amplitude. Note that the discrete modes of $\mathcal{S}$ will not have any momentum quantum number, but they can interact directly with discrete modes like two-level systems in $\mathcal{M}_2$. One can also have processes in which $\mathcal{S}$ interacts with a two-level system which then recoils (thereby emitting a phonon).

As already noted, in reality the surface will not have the idealized flat surfaces shown [Fig. 5(b) exaggerates these irregularities somewhat]. When the wavelength $\lambda = \hbar/M_o v$ of the center-of-mass coordinate of $\mathcal{S}$, moving at velocity v, satisfies $\lambda \ll a_o, b_o$, then the scattering will be sensitive to these irregularities, so that two given objects $\mathcal{S}$ and $\mathcal{S}'$ coming in with identical $(\epsilon, \mathbf{k})$, but different impact parameters, will be scattered differently. On the other hand, for low-energy electrons $\lambda \gg a_o, b_o$, so that surface irregularities will be unimportant.

As already noted, we will reject any experimental design for massive objects (such that $\lambda \ll a_o, b_o$) if surface irregularities do play any role.

The decoherence mechanisms just discussed are distinct from those that are the prime focus of this paper: but in any experiment they will also contribute, and their detailed theoretical treatment will obviously be complicated. To get some idea of how things may work, we now consider the two examples of interest, in turn.

B. Electron interferometry

We begin with electrons, which have a very low mass, and hence long wavelength. In early discussions of the two-slit system, going back to Heisenberg, Einstein, and Bohr, the actual electron-slit interaction is not analyzed. One instead simply assumes total momentum conservation so that the deviation in the electron path as it goes through one or the other slit is accompanied by a recoil of the slit system. This analysis, however, does not allow us to say anything about the photon-mediated electron decoherence, which depends in principle on the detailed path of the electron (and, in particular, the acceleration it undergoes).

We can certainly make a crude estimate of the photon-mediated decoherence rate, by noting that for the geometry shown in Fig. 4, one can assume that the electron acceleration, caused by interaction with the slits, takes place over a length scale $\sim a_o$, the thickness of the plates in which the slits are situated. Then, if the slit-screen distance is L_o, and the distance between the slits is d_o, the acceleration suffered by the electron as it passes through one or other of the slits is given by

$$a_j \sim \frac{\delta v_j}{\delta t} \sim \frac{v^2}{\ell_o}\theta_j \sim \frac{v^2}{\ell_o}\left(z_f \pm \frac{1}{2}d_o\right), \tag{46}$$

where $j = A, B$ labels the two paths for the electron, z_f is the final position (on the $\hat{z}$ axis) of the electron on the screen, θ_j is the angle through which the electron is deflected on the jth path, and v is the electron velocity as before.

In this case the the frequency $\Omega = 1/\Delta t$, where $\Delta t = a_o/v$ is just the time taken for the electron to pass through the interaction region, and the "coarse-graining" length scale l_0 defined above can also be taken to be a_o (in conventional units).

Let us consider a charged particle with charge Qe, where e is the electronic charge. Restoring the units to MKS (Metre-Kilogram-Second) units, so that the fine structure constant $\alpha = \frac{e^2}{4\pi}$, we then have, for this experiment, the following predictions from Eqs. (38) and (45) for the decoherence rates:

$$\Gamma_{\rm dressed} \sim Q^2 \frac{16\alpha}{3\pi}\left(\frac{v}{c}\right)^2 \ln(L_o/a_o), \tag{47}$$

$$\Gamma_{\rm hard} \sim Q^2 \frac{8\alpha}{3\pi}\left[2\ln(L_o/a_o) + \frac{1}{2}(L_o/a_o)^2\right]. \tag{48}$$

Are these estimates changed by a more sophisticated analysis? It turns out that this is not a simple question: the mechanism by which momentum and energy is exchanged between the electron, the slit system, and photons is still being debated [60]. Here we give our point of view.

In a real two-slit system, the electron polarizes the two-slit system as it approaches it; this polarization can be understood, and the electron-slit interaction can be written in terms of the dielectric function of the slit system [61]. However, electrons that succeed in propagating through the slits will not typically make contact with $\mathcal{M}_2$ (if they do, then their paths will be severely disturbed, and they are likely to stick to or be absorbed on the surface of $\mathcal{M}_2$).

In reality the electrons will interact indirectly with the slit system through their interaction with the electric fields which exist in the vicinity of the slits [60,62]. To treat this problem properly requires detailed treatment of both the static and fluctuating electromagnetic fields in and around the slits: it is actually an example of the "Casimir" problem for this geometry [63].

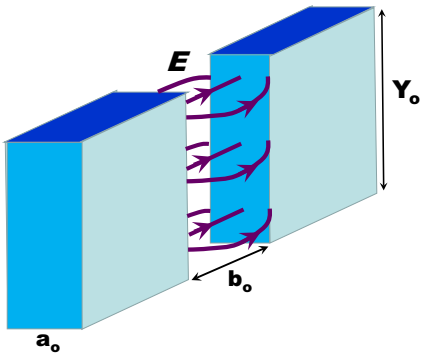

FIG. 6. Depiction of the electric field configuration around a slit in a dielectric slit system $\mathcal{M}_2$. In a quantum treatment, local photon modes exist in this region, and an incoming electron can scatter such bound-state modes between different energy levels.

It is well known that a proper treatment of even a simple geometry for such Casimir problems, for a general dielectric material making up the slits, is extremely complex. A simplified treatment [62] starts from the classical "open cavity" electromagnetic modes in the slit region, comprising both localized modes confined to within the slits, and evanescent modes extending away from the slits.

To see how this works, consider the geometry shown in Fig. 6, in which the slits have width b_o, length Y_o, and thickness a_o. Then the localized modes, confined to the slit region, have electric fields of form [62]

$$E_z(x, y) = E_o \sin\left(\frac{\pi y}{Y_o}\right)\frac{\cosh\kappa_\omega x}{\cosh\left(\frac{1}{2}\kappa_\omega a_o\right)}, \tag{49}$$

where the wave vector κ_ω is given by

$$\kappa_\omega^2 = \left(\frac{\pi}{Y_o}\right)^2 - \frac{\omega^2}{c^2}. \tag{50}$$

We then end up with a set of photon bound states in the slit region, which, when quantized, are populated thermally by photons. Quantized momentum exchange between the electron and the slit photon modes then leads to deviation of the electron path as it travels through the slit, accompanied by multiple transitions of photons between the bound-state levels. The details are rather lengthy in the general case [62], but the key conclusion is that in situations where photons in many different levels are arrived, one recovers the results given above for the photon-mediated decoherence rate.

Finally, let us note that in any real experiment the photon bath will be at some finite temperature T. One can in fact generalize all of the calculations in the previous sections of this paper to finite T. Since the basic methods for doing this are well known (see, e.g., Refs. [64,65] for general discussions), we simply give the main results here.

The easiest way to set up this kind of calculation is to define a decoherence functional [50,51] for the effect of a finite-T photon bath on the electron dynamics [9,25]. This

then modifies Eq. (14) to

$$\Gamma[j_L, j_R] = \frac{1}{2}\int \frac{d^3q}{(2\pi)^3 2\omega} P_{ab} \coth(\beta\omega/2)\, \delta j^a(q)\delta j^b(-q), \tag{51}$$

where $\beta = 1/kT$, and we now have to assume a specific reference frame in which the photon bath, at equilibrium temperature T, is at rest; this will usually be determined by the two-slit system itself, which is assumed to be in equilibrium with the photon bath. We note that the same $\coth(\beta\omega/2)$ factor will enter into the integrals in, e.g., Eqs. (25), (36), (37), (39), and (44).

The essential physical effect of the temperature factor here is to introduce a new energy scale in the problem. If $kT \ll \Omega$ this becomes a new IR energy scale; in the opposite case where $kT \gg \Omega$ the electrons are simply interacting with a high-temperature photon bath.

Finally, one can ask about other decoherence sources in this experiment. In fact these will be rather small for a slow-moving electron; the available phase space for phonon creation will be extremely small at energies equal to the electron kinetic energy. For an electron moving at $v = 10^3$ m/s having wavelength $\lambda \sim 10^{-7}$ m, this energy is ~40 mK, and correspondingly much less for lower velocities. There will also be possible decoherence from electron spin-flip processes, mediated by paramagnetic impurities in the slit system, which for well-prepared slit systems can be neglected.

We thus conclude that the results found in Eqs. (38) and (45), for photon-mediated decoherence, are in principle measurable.

C. Electron interferometry with massive particles

There are well-known experiments [66] in which rather massive molecules are used instead of electrons in two-slit experiments. However, any attempt to analyze these theoretically is very complicated [43] because the molecules have irregular shape, and in general carry angular momentum. Both the angular momentum and the internal "shape" degrees of freedom of the molecule (modeled by vibrational and "twisting" modes, amongst others) can couple to the slit system [6], and this leads to extra sources of "third-party decoherence" (since the coupling to these degrees of freedom depends on which path the object takes).

The key differences between such experiments and the electron interference experiments described above are (i) the much larger mass and energy, and much shorter wavelength, associated with the center of mass; (ii) the much larger role of other kinds of environmental decoherence; and (iii) the possibility of using neutral (dielectric) particles; even a neutral object still interacts with photons if its dielectric properties are different from the vacuum.

In the following we will only consider electrically neutral particles; if the particle is charged, we can adapt the previous results for the electron to estimate the photon decoherence.

In all cases, what we wish to know is how does the photon decoherence compare with other environmental sources of decoherence? There are many different possible situations; here we summarize some key ideas.

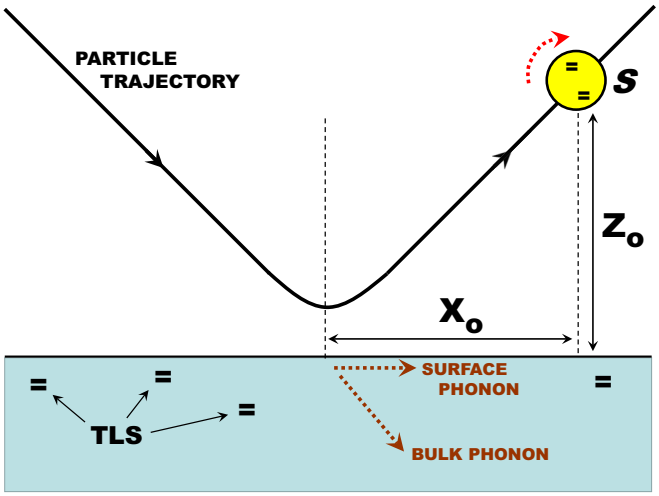

FIG. 7. Interaction of a massive spherical particle, of radius r_o, with a flat mirror. The coordinates of the center of mass of the particle relative to the origin are $(X_o, Y_o, Z_o + r_o)$; the particle is moving in the $\hat{x}$ direction. The interaction will generate phonons in the mirror and vibrational and rotational motion in the particle. Two-level systems and spins in the particle can interact with those in the mirror via dipolar interactions.

1. Basic design

We rely in what follows on the experimental possibility of almost elastic reflection of a slow-moving particle from a flat mirror. If both the mirror and the particle are electrically neutral, then the interaction between them is well known to be a combination of a short-range repulsion between atoms and a long-range van der Waals attraction. This experiment is shown schematically in Fig. 7. If the particle is charged, then the charge will also induce a mirror charge on the mirror. If the particle and mirror are conducting we have a quite different situation again. Such problems have been studied for many years [67–70].

The most conceptually simple case is of perfectly conducting (but uncharged) particle and mirror; then the following results are known to be the case:

(i) When the particle is far from the plane, so that $Z_o \gg r_o$, one has the asymptotic relativistic van der Waals behavior

$$V_o(Z_o) \sim U(Z_o) - \frac{9\hbar c}{16\pi}\frac{r_o^3}{(r_o + Z_o)^4} \quad (Z_o \gg r_o), \tag{52}$$

where $U(Z_o)$ is a short-range interaction, which in this simple model takes the form $U(Z_o) = U_o\theta(-Z_o)$.

(ii) On the other hand when $Z_o \ll r_o$ one finds [71]

$$V_o(Z_o) \sim U(Z_o) + \left(\frac{1}{3} - \frac{5}{\pi^2}\right)\frac{\hbar\pi^3 c}{720}\frac{1}{Z_o}. \tag{53}$$

In the intermediate range one has $[V_o(Z_o) - U(Z_o)] \sim O(1/Z_o^3)$ (the long-range nonrelativistic van der Waals behavior).

In this simple example one already sees the key difference between the two parts of $V_o(Z_o)$. The long-range van der Waals term can be determined via macroscopic considerations (although it can depend in a very complicated way on the shape

and material properties of the two bodies). This physics has been studied in considerable detail [71].

The result for the short-range $U(Z_o)$, on the other hand, is just the standard Casimir result for perfect conductors. However, it is extremely unrealistic for any real conducting system. In reality, a close approach between two large systems like this brings into play physics at atomic length scales, and energies as much as hundreds of eV. When a massive particle approaches a surface with appreciable kinetic energy, a serious distortion of the surface regions of both particle and surface ensues during the collision, involving the surface and also layers well below the surface, so that $U_o(Z_o)$ operates indirectly over length scales ranging from atomic scales up to several nanometers. Simulations of even quite simple examples [72] show that this process is highly complex. In real systems the collision can also create defects and dislocations, or move existing ones around (and as noted, on macroscopic length scales this is seen as a patch potential [58]). It can also involve severe disturbances of the outer shells of atoms, including ionization, with the liberation of photons.

Thus, for any real system, the physics for a large particle approaching a plane is extraordinarily complex. The simple model of a perfectly conducting system, while being a nice simple model to analyze, is far from being realistic. We can instead make progress here by considering the interaction between a solid spherical dielectric and a solid semi-infinite dielectric system restricted to a half-plane. We assume again that the closest distance between the sphere, of radius r_o, and the solid half-plane, is Z_o.

We begin with an action of form

$$S[\mathbf{R}_o, h_\mathbf{q}] \;=\; S_o[\mathbf{R}_o] + S_{\rm surf}[h_\mathbf{q}] + S_{\rm int}[\mathbf{R}_o, h_\mathbf{q}], \tag{54}$$

where $h_\mathbf{q}$ is the Fourier transform of the height fluctuations of the mirror surface, i.e., where $h(\mathbf{r}_\perp, t) = h_\mathbf{q} e^{i(\mathbf{q}\cdot\mathbf{r}_\perp - \omega t)}$, with a displacement $\mathbf{r}_\perp$ on the surface relative to the origin. The particle center-of-mass coordinate is $\mathbf{R}_o = (Z_o + r_o, X_o)$ relative to the same origin on the surface. The various terms in $S[\mathbf{R}_o, h_\mathbf{q}]$ are then

$$\begin{aligned} S_o[\mathbf{R}_o] \;&=\; \frac{1}{2}\int dt [M_o \dot{R}_o^2 - V(Z_o)], \\ S_{\rm surf}[h_\mathbf{q}] \;&=\; \frac{1}{2}\int dt \left[\frac{\rho_o}{q}\left(\dot{h}_\mathbf{q}^2 - \omega_\mathbf{q}^2 h_\mathbf{q}^2\right)\right], \\ S_{\rm int}[\mathbf{R}_o, h_\mathbf{q}] \;&=\; -\int dt \sum_\mathbf{q} \lambda_\mathbf{q}(\mathbf{R}_o) h_\mathbf{q}, \end{aligned} \tag{55}$$

where ρ_o is the density of the mirror, and $\omega_\mathbf{q}$ is the dispersion for the surface waves of the mirror: there will be two branches coming from longitudinal and transverse surface phonons. To find the interaction $\lambda_\mathbf{q}(\mathbf{R}_o)$ one assumes [73] a van der Waals interaction $-g_o/|\mathbf{r} - \mathbf{r}'|^6$ between unit volumes of dielectric situated at $\mathbf{r}, \mathbf{r}'$.

Integrating over the sphere and the mirror [73,74], introducing oscillator coordinates

$$x_\mathbf{q} \;=\; (\hbar/2m_q\omega_\mathbf{q})^{1/2} h_\mathbf{q}, \tag{56}$$

we can finally write the effective action for the particle-mirror system as $S_{\rm eff} = \int dt\, L_{\rm eff}$, where $L_{\rm eff}$ has the Caldeira-Leggett form

$$L_{\rm eff} = \frac{1}{2}M_o\dot{R}_o^2 - V(Z_o) + \frac{1}{2}\sum_\mathbf{q} m_q\left(\dot{x}_\mathbf{q}^2 - \omega_q^2 x_\mathbf{q}^2\right) - \tilde{\lambda}_\mathbf{q}(\mathbf{R}_o)x_\mathbf{q} \tag{57}$$

in which the coupling takes the final form

$$\tilde{\lambda}_\mathbf{q}(\mathbf{R}_o) \;=\; -\frac{2^{1/2}\pi^2}{3} r_o^3 g_o \frac{q^2}{Z_o^2} K_2(qZ_o)\cos(qX_o). \tag{58}$$

With this result one can calculate phonon decoherence for some path of the particle [73,74]. To find the photon decoherence, one derives a similar action for the coupling to photons. Let us now briefly consider what one expects for the different contributions to the decoherence.

2. Contributions to decoherence

As already noted, if the massive particle is charged, we can estimate photon decoherence using the results given for the simple electron. Here we focus on the neutral particle discussed above.

To properly formulate this problem, we note that the electrodynamic properties of the neutral particle are described by a dielectric function $\varepsilon(\mathbf{q}, \omega)$. At the energy scales of interest here, the photon wavelength $\lambda = 1/|\mathbf{q}| \gg r_o$, and the effective interaction between photons and the moving particle will be proportional to its dielectric polarizability $\alpha_p \sim O(\varepsilon_o r_o^3)$. This gives a (Rayleigh) scattering rate $\Lambda_\mathbf{q} \propto |\mathbf{q}|^4\alpha_p^2$; for a dielectric sphere, having no dielectric moment, one has [75]

$$W_\mathbf{q}^{\rm EM} \;=\; \frac{8\pi}{3}\left(\frac{\varepsilon - 1}{\varepsilon + 2}\right)^2 \varepsilon_o r_o^6 |\mathbf{q}|^4, \tag{59}$$

where ε is the long-wavelength limit of $\varepsilon(\mathbf{q}, \omega)$.

Both the decoherence from scattering off photons, and that from their absorption and emission, are then determined by $W_\mathbf{q}^{\rm EM}$; insertion of this scattering rate into the decoherence functional (51) now gives a decoherence rate $\propto r_o^6 d\omega\, \omega^5 \coth(\beta\omega/2)$, which is rather small at low T, and which must compete with the decoherence from both phonons and defects.

The phonon decoherence rate from the coupling surface phonons can be calculated directly [76] from the form of the coupling given above in (58); this yields a decoherence rate $\propto r_o^6 d\omega\, \omega^3 \coth(\beta\omega/2)$, which then dominates over the photon decoherence rate at low T.

Finally, one can discuss the decoherence coming from defects and paramagnetic impurities in the particle-mirror system. Quite generally one can discuss this using the spin bath representation of these objects [44]. Typically they will interact via dipolar interactions (electric or magnetic), and one can write an influence functional for their effect on the particle decoherence; we forego the details here.

From all this we can conclude several things: If one is to stand any chance of seeing and measuring the photon decoherence for such neutral particles, we must be able to separate it from the phonon and defect contributions, and the phonon contribution will typically be much larger. To minimize phonon emission, and to rule out inelastic deformation of the surfaces, the kinetic energy of the massive particle has

to be low, low enough so that the phonon excitation rate is controllable. Roughly speaking, we would like this kinetic energy to be ∼1 eV or less, and the energy exchange between the particle and the surface needs to be hundreds of times lower.

To get an idea of the numbers, we note that for a SiO_2 particle of mass $M_o = 2 \times 10^4$ AMU, containing 167 SiO_2 units, and having diameter ∼2 nm, a kinetic energy of 1 eV is attained when $v = 100$ m/s; for a particle of mass $M_o = 2 \times 10^8$ AMU, containing 1.67×10^6 SiO_2 units, and having diameter ∼40 nm, a kinetic energy of 1 eV is attained when $v = 1$ m/s. Now note that the length scale over which the particle "bounces" will be $\sim O(r_o)$, thereby involving times $\Delta t \sim r_o/v$ and frequencies $\Omega \sim v/r_o$; for the two examples just given, we have $\Omega \sim 10^{11}$ Hz for the small particle (i.e., μwaves), and $\Omega \sim 5 \times 10^7$ Hz (i.e., RF), for the large particle.

We can therefore conclude by saying that the best kind of experiment to look at soft-photon decoherence is very likely the two-slit experiment with electrons, or some similar design. A proper comparison of theory and experiment will require detailed consideration of the electron-slit interaction, as well as quantifying contributions from other decoherence sources.

VIII. DISCUSSION

The presence of infrared divergences demanded that we apply infrared dressing at leading order. Our view on the status of possible *subleading* dressing, however, is still murky. While the leading and subleading currents have much in common classically, quantum mechanically only the former contributes to obviously unphysical conclusions. Accordingly, we have speculated here about whether it might be possible to observe subleading soft dressing (or its absence) using an interferometer.

Interpreting the subleading contribution (43) to decoherence is mostly straightforward. The full electromagnetic field obtains an amount of which-path information given by (38). The amount of this information attributable solely to the difference between the subleading soft radiation emitted by each branch of the matter superposition is given by (43), which shows that the subleading soft contribution grows quadratically in l, the size of the interferometer. This makes sense because subleading soft photons are by definition excitations of the electromagnetic field with a very long wavelength, and are capable of resolving only large-scale details of the matter system. The interpretation of (43) is then as follows: the larger the matter system, the more capable subleading soft photons are of making quantum measurements of it. For larger experiment geometries, more of the quantum information broadcast by the charged particle then ends up being stored in subleading soft modes, relative to the hard modes. Keep in mind of course that we have obtained our results using the dipole approximation, in which we assume that the wavelength of any emitted radiation is still much larger than the size of the experiment. It would be interesting to go beyond this approximation in future work.

We should also at this point caution the reader that we do not regard our discussion, here and in in Sec. VI C, to be complete. The soft currents $j^a_{\rm div}$ and $j^a_{\rm sub}$ have been shown [41] to encode the leading and subleading soft-photon theorems *at tree level*. While the leading soft-photon theorem is already exact at tree level, the subleading soft-photon theorem in general receives loop corrections [77–80]. It then would be prudent to explore quantum corrections to our simple semiclassical model, if we hope to fully understand whether any subleading dressing is required, and what form it might take. In the meantime, as in other discussions of subleading soft dressing [39], our results beyond leading soft order may be trusted up to $O(e^2)$ in a perturbative expansion. We therefore conclude that the issue of the dressing of subleading contributions requires both more theoretical work and experimental testing.

Finally, we note that the framework presented here can likely be extended to other physical systems. In particular, it would be of interest to apply these techniques, along the lines of our previous work [41], to a straightforward extension to the study of leading, subleading, and sub-subleading [81] soft graviton radiation.

ACKNOWLEDGMENT

We thank J. Wilson-Gerow for discussions of this work, which was supported by NSERC in Canada.

APPENDIX A: DRESSING, IN DETAIL

In this Appendix, we will illustrate the usual "dressed" formalism [26–31] using a scattering amplitude involving only a single charged particle in QED. This simple example suffices for our needs since our interferometry model too involves only a single charged particle. We then show how the dressing works in our finite-time model, proving that a minimal form of infrared dressing can be accomplished simply by setting the divergent soft current $j^a_{\rm div}$ to zero everywhere.

1. Dressed scattering

In textbook QED, the scattering amplitude for a charged particle to transition from the momentum eigenstate $|p_i\rangle$ to the momentum eigenstate $|p_f\rangle$, while the photon field transitions from $|\alpha\rangle$ to $|\beta\rangle$ is

$$\langle p_f, \beta|\hat{S}|p_i, \alpha\rangle, \tag{A1}$$

where $\hat{S}$ is the QED S matrix. Applying infrared dressing to this formalism amounts to making the replacement

$$\langle p_f, \beta|\hat{S}|p_i, \alpha\rangle \to \langle p_f, \beta|e^{-\hat{R}_f}\,\hat{S}\,e^{\hat{R}_i}|p_i, \alpha\rangle, \tag{A2}$$

where the "dressing operator," which acts on the photon Hilbert space, is

$$\hat{R}_{i/f} \equiv \sum_{h=+,-}\int \frac{d^3q}{(2\pi)^3\sqrt{2\omega}}\left[F^h_{i/f}(q)\hat{a}^\dagger_h(q) - \bar{F}^h_{i/f}(q)\hat{a}_h(q)\right], \tag{A3}$$

in which $\hat{a}^\dagger_h(q)$ and $\hat{a}_h(q)$, respectively, create and annihilate a photon with momentum $q^a \equiv \omega(1, \hat{n})$ and helicity h, and obey

$$[\hat{a}_h(q), \hat{a}^\dagger_{h'}(q')] = \delta_{hh'}(2\pi)^3\delta^{(3)}(\vec{q} - \vec{q}'). \tag{A4}$$

We have also defined

$$F^h_{i/f}(q) \equiv e\frac{\epsilon_h(q)\cdot p_{i/f}}{q\cdot p_{i/f}}\,\phi(q, p_{i/f}), \tag{A5}$$

with ϵ_h^a the polarization vector corresponding to the helicity h, and $\phi(q, p)$ may be chosen arbitrarily, except that it must go smoothly to 1 as $|\vec{q}| \to 0$ in order for the dressing to properly remove the infrared divergence we saw in the main text.

To remove the divergence, then, it suffices to choose $\phi(q, p)$ nonzero only in a neighborhood of $|\vec{q}| = 0$, where the divergence occurs. Such a choice would, however, necessitate the introduction of at least one new parameter, an arbitrary new energy scale "Λ," to our model, in order to characterize the size of the momentum neighborhood involved in the dressing. There is no physical energy scale in our interferometry model with which we could identify Λ, so instead we make a more conservative choice involving no new parameters at all, simply letting

$$\phi(q, p) = 1, \tag{A6}$$

a choice which has been referred to elsewhere as "minimal" dressing [40]. With this choice, the frequency integral in (A3) should be understood as extending from the infrared cutoff λ up to the ultraviolet cutoff Ω, with λ eventually being taken to zero. We will use this choice of $\phi(q, p)$ in what follows, and we will see that the minimal dressing has a very clean interpretation in terms of the infrared-divergent soft-matter current $j^a_{\rm div}$, making it a natural choice in light of the deep interplay between the soft currents and infrared radiation [41].

Evolving states using the dressed S matrix $e^{-\hat{R}_f}\hat{S}\,e^{\hat{R}_i}$ instead of the bare S matrix $\hat{S}$ allows one to avoid unphysical infrared-divergent decoherence rates. This has been shown already in scattering calculations [32], and we will now show how it works in our finite-time interferometry model. In particular we want to dress the interaction picture time-evolution operator, which we used in Eq. (4), as

$$\mathcal{T}e^{-i\int d^4x\, j^a(x)\hat{A}_a(x)} \to e^{-\hat{R}_f}\left[\mathcal{T}e^{-i\int d^4x\, j^a(x)\hat{A}_a(x)}\right]e^{\hat{R}_i}, \tag{A7}$$

with $\hat{R}_{i/f}$ given by (A3), but now with the factors $F^h_{i/f}(q)$ of (A5) evaluated at the beginning and end of the interferometry experiment (at proper times $s_{i/f}$), rather than at the asymptotic times $t \to \pm\infty$ relevant in scattering scenarios. We will now show that in order to effect minimal dressing, using (A6), we need only set the divergent part $j^a_{\rm div}$ of the electromagnetic current j^a appearing here to zero. That is, we will show that

$$e^{-\hat{R}_f}\left[\mathcal{T}e^{-i\int d^4x\, j^a(x)\hat{A}_a(x)}\right]e^{\hat{R}_i} = \mathcal{T}e^{-i\int d^4x\,[j^a - j^a_{\rm div}](x)\hat{A}_a(x)}. \tag{A8}$$

The mechanism by which minimal infrared dressing removes infrared divergences is thus the wholesale decoupling of the Maxwell field from the infrared-divergent soft current $j^a_{\rm div}$.

2. Minimal dressing removes the divergent soft current

To prove Eq. (A8), let us begin with the second line and work our way backward. The second term in the exponent there is

$$i\int d^4x\, j^a_{\rm div}(x)\hat{A}_a(x), \tag{A9}$$

with $j^a_{\rm div}$ defined by Eq. (23). Using the mode expansion of $\hat{A}_a(x)$,

$$\hat{A}_a(x) = \sum_{h=+,-}\int \frac{d^3q}{(2\pi)^3\sqrt{2\omega}}\left[\epsilon^h_a\hat{a}^\dagger_h(q)e^{iq\cdot x} + \bar{\epsilon}^h_a\hat{a}_h(q)e^{-iq\cdot x}\right], \tag{A10}$$

we can rewrite (A9) as

$$\begin{aligned} &i\int d^4x\, j^a_{\rm div}(x)\sum_{h=+,-}\int \frac{d^3q}{(2\pi)^3\sqrt{2\omega}}\left[\epsilon^h_a\hat{a}^\dagger_h e^{iq\cdot x} + \bar{\epsilon}^h_a\hat{a}_h e^{-iq\cdot x}\right] \\ &\quad = i\sum_{h=+,-}\int \frac{d^3q}{(2\pi)^3\sqrt{2\omega}}\left[\epsilon^h_a\hat{a}^\dagger_h j^a_{\rm div}(q) + \bar{\epsilon}^h_a\hat{a}_h j^a_{\rm div}(-q)\right] \\ &\quad = \sum_{h=+,-}\int \frac{d^3q}{(2\pi)^3\sqrt{2\omega}}\left[\bar{\epsilon}^h_a\hat{a}_h - \epsilon^h_a\hat{a}^\dagger_h\right]\frac{\dot{X}^a(s_f)}{q\cdot\dot{X}(s_f)} \\ &\qquad - (s_f \to s_i). \end{aligned} \tag{A11}$$

Comparing to Eqs. (A3) and (A5), this is nothing but

$$-\hat{R}_f + \hat{R}_i, \tag{A12}$$

with $p^a_{i/f} = m\dot{X}^a(s_{i/f})$ and the choice of minimal dressing $\phi(q, p) = 1$.

This result allows us to conclude that

$$\mathcal{T}e^{-i\int d^4x\,[j^a - j^a_{\rm div}](x)\hat{A}_a(x)} = \mathcal{T}e^{-i\int d^4x\, j^a(x)\hat{A}_a(x) - \hat{R}_f + \hat{R}_i}. \tag{A13}$$

We can rewrite this using the form (3) of the position space current $j^a(x)$ as

$$\mathcal{T}e^{-ie\int_{s_i}^{s_f} ds\,\dot{X}^a(s)\hat{A}_a[X(s)] - \hat{R}_f + \hat{R}_i}, \tag{A14}$$

in order to see explicitly that the time ordering of operators using the coordinate time t gives the same result as ordering operators using the proper time s. Because the dressing operators here act at the beginning and end of the experiment, i.e., $\hat{R}_{i/f}$ contains a contribution only when the proper time is $s_{i/f}$, we can thus pull $\hat{R}_f$ out from under the time-ordering operator $\mathcal{T}$ to the left, and we can pull $\hat{R}_i$ out to the right, leaving

$$e^{-\hat{R}_f}\left[\mathcal{T}e^{-ie\int_{s_i}^{s_f} ds\,\dot{X}^a(s)\hat{A}_a(X(s))}\right]e^{\hat{R}_i} \tag{A15}$$

or, equivalently,

$$e^{-\hat{R}_f}\left[\mathcal{T}e^{-i\int d^4x\, j^a(x)\hat{A}_a(x)}\right]e^{\hat{R}_i}, \tag{A16}$$

proving Eq. (A8).

APPENDIX B: INTEGRALS

This Appendix includes further detail on the evaluation of the dressed decoherence functional $\Gamma_{\rm dressed}$, and the subleading soft and hard contributions $\Gamma_{\rm sub}$ and $\Gamma_{\rm hard}$ to this, which are defined in the main text. Our approach to these calculations is similar to that of Breuer and Petruccione [9].

1. Dressed decoherence functional

First write $\Gamma_{\rm dressed}$ [Eq. (37)] as

$$\Gamma_{\rm dressed} \equiv \frac{e^2}{(2\pi)^3}\mathcal{I}_\omega\mathcal{I}_{\hat{n}} \tag{B1}$$

with

$$\mathcal{I}_\omega \equiv 2\int_0^\Omega d\omega\,\frac{(1-\cos\omega\tau)}{\omega} \tag{B2}$$

and

$$\mathcal{I}_{\hat{n}} \equiv \oint dS^2(\hat{n})\,\omega^2\left[2\frac{\dot{X}_1\cdot\dot{X}_2}{(q\cdot\dot{X}_1)(q\cdot\dot{X}_2)} - \frac{1}{(q\cdot\dot{X}_1)^2} - \frac{1}{(q\cdot\dot{X}_2)^2}\right]. \tag{B3}$$

We will evaluate each of these integrals one at a time.

The frequency integral $\mathcal{I}_\omega$ can be written as (using $\varpi \equiv \omega\tau$)

$$2\int_0^{\Omega\tau} d\varpi\,\frac{(1-\cos\varpi)}{\varpi}. \tag{B4}$$

We can then use the following identity [82] involving the cosine integral:

$$\begin{aligned}\mathrm{Ci}(\Omega\tau) &\equiv -\int_{\Omega\tau}^\infty d\varpi\,\frac{\cos\varpi}{\varpi}\\ &= \gamma_{\mathrm{EM}} + \ln\Omega\tau - \int_0^{\Omega\tau} d\varpi\,\frac{(1-\cos\varpi)}{\varpi},\end{aligned} \tag{B5}$$

where $\gamma_{\mathrm{EM}} \approx 0.577$ is the Euler-Mascheroni constant, from which it follows that $\mathcal{I}_\omega$ is

$$2\int_0^{\Omega\tau} d\varpi\,\frac{(1-\cos\varpi)}{\varpi} = 2[\gamma + \ln\Omega\tau - \mathrm{Ci}(\Omega\tau)]. \tag{B6}$$

In the limit $\Omega\tau \gg 1$ discussed in the main text, the logarithm dominates this expression, giving the approximate result

$$\mathcal{I}_\omega \approx 2\,\ln\Omega\tau. \tag{B7}$$

The angular integral $\mathcal{I}_{\hat{n}}$ is a sum of three terms with integrals of the form

$$\begin{aligned}&\oint dS^2(\hat{n})\,\omega^2\frac{\dot{X}_A\cdot\dot{X}_B}{(q\cdot\dot{X}_A)(q\cdot\dot{X}_B)}\\ &\quad= \oint dS^2(\hat{n})\,\frac{(1-\vec{v}_A\cdot\vec{v}_B)}{(1-\hat{n}\cdot\vec{v}_A)(1-\hat{n}\cdot\vec{v}_B)},\end{aligned} \tag{B8}$$

with $A, B \in \{1, 2\}$. The Lorentz invariance of this integral allows us to evaluate it in any reference frame. For convenience we can choose the frame in which $\vec{v}_B = 0$, bringing $\mathcal{I}_{\hat{n}}$ into the simple form

$$\oint dS^2(\hat{n})\,\frac{1}{(1-\hat{n}\cdot\vec{v}_{AB})} = \frac{4\pi}{v_{AB}}\tanh^{-1} v_{AB}, \tag{B9}$$

where v_{AB} is the relative velocity,

$$v_{AB} \equiv \sqrt{1 - \frac{1}{(\dot{X}_A\cdot\dot{X}_B)^2}}. \tag{B10}$$

We can use the result (B9) to see that the angular integral (B3) is

$$\mathcal{I}_{\hat{n}} = 8\pi\left[\frac{1}{v_{12}}\tanh^{-1} v_{12} - 1\right]. \tag{B11}$$

In the geometry illustrated in Fig. 2, the relative velocity v_{12} is approximately

$$v_{12} \approx \sqrt{2}v, \tag{B12}$$

in the case of nonrelativistic speeds, $v \ll 1$, where again $v \equiv l/\tau$. We can further approximate

$$\frac{1}{v_{12}}\tanh^{-1} v_{12} = 1 + \frac{1}{3}v_{12}^2 + \cdots \approx 1 + \frac{2}{3}v^2. \tag{B13}$$

In this limit, the angular integral is

$$\mathcal{I}_{\hat{n}} \approx \frac{16\pi}{3}v^2. \tag{B14}$$

Plugging Eqs. (B7) and (B14) into (B1) yields Eq. (38):

$$\Gamma_{\mathrm{dressed}} \approx \frac{4e^2v^2}{3\pi^2}\ln\Omega\tau. \tag{B15}$$

2. Subleading soft contribution to the decoherence functional

The subleading soft part of the dressed decoherence functional, given by Eq. (39), can also be written in the form of a frequency integral multiplied by an angular integral:

$$\Gamma_{\mathrm{sub}} \equiv \frac{e^2}{(2\pi)^3}\mathcal{I}_\omega^{\mathrm{sub}}\mathcal{I}_{\hat{n}}. \tag{B16}$$

Here, the angular integral $\mathcal{I}_{\hat{n}}$ is the same one we have already evaluated, so we can simply use the result (B14). The frequency integral is different, however; we have

$$\mathcal{I}_\omega^{\mathrm{sub}} \equiv \int_0^\Omega d\omega\,\omega\tau^2 = \frac{1}{2}\Omega^2\tau^2. \tag{B17}$$

Plugging these results into (B16) gives the result (42):

$$\Gamma_{\mathrm{sub}} \approx \frac{e^2}{3\pi^2}\Omega^2v^2\tau^2. \tag{B18}$$

3. Hard contribution to the decoherence functional

The hard part of the decoherence functional, obtained by "dressing" away both the leading and subleading currents, is given by Eq. (44). As before, this decoherence functional may also be written in the form of a frequency integral multiplied by an angular integral:

$$\Gamma_{\mathrm{hard}} \equiv \frac{e^2}{(2\pi)^3}\mathcal{I}_\omega^{\mathrm{hard}}\mathcal{I}_{\hat{n}}. \tag{B19}$$

Again, the angular integral $\mathcal{I}_{\hat{n}}$ is the same as before, and we will reuse the result (B14). The frequency integral in this case is

$$\begin{aligned}\mathcal{I}_\omega^{\mathrm{hard}} \equiv \int_0^\Omega \frac{d\omega}{\omega}\,&(2 - 2\,\cos\omega\tau + i\omega\tau e^{i\omega\tau}\\ &- i\omega\tau e^{-i\omega\tau} + \omega^2\tau^2).\end{aligned} \tag{B20}$$

Comparing to Eqs. (B2) and (B17), we see that $\mathcal{I}_\omega^{\mathrm{hard}}$ can be written as

$$\mathcal{I}_\omega^{\mathrm{dressed}} + \mathcal{I}_\omega^{\mathrm{sub}} - \int_0^\Omega d\omega\,(i\tau e^{i\omega\tau} - i\tau e^{-i\omega\tau}), \tag{B21}$$

allowing us to reuse more of our previous results. Doing so, and evaluating the new integral in the third term gives

$$\mathcal{I}_\omega^{\mathrm{hard}} = 2[\gamma + \ln\Omega\tau - \mathrm{Ci}(\Omega\tau)] + \tfrac{1}{2}\Omega^2\tau^2 + 2[1 - \cos\Omega\tau]. \tag{B22}$$

Only two terms here contribute significantly when $\Omega\tau \gg 1$, leaving

$$\mathcal{I}_{\omega}^{\text{hard}} \approx 2\,\ln\Omega\tau + \tfrac{1}{2}\Omega^2\tau^2. \tag{B23}$$

Plugging these results into (B19) yields

$$\Gamma_{\text{hard}} \approx \frac{2e^2}{3\pi^2}v^2\left[2\,\ln\Omega\tau + \frac{1}{2}\Omega^2\tau^2\right], \tag{B24}$$

in agreement with Eq. (45).

[1] R. P. Feynman, R. B. Leighton, and M. Sands, *The Feynman Lectures on Physics* (Addison-Wesley, Boston, 1965), Vol. 3.

[2] To rigorously divide the matter paths into discrete classes requires a little work; see A. Auerbach, S. Kivelson, and D. Nicole, Path decomposition for multidimensional tunneling, Phys. Rev. Lett. **53**, 411 (1984); A. Auerbach and S. Kivelson, The path decomposition expansion and multidimensional tunneling, Nucl. Phys. B **257**, 799 (1985), for nonrelativistic discussions appropriate to, e.g., a two-path system.

[3] E. Joos and H. D. Zeh, The emergence of classical properties through interactions with the environment, Z. Phys. B **59**, 223 (1985).

[4] E. Joos, H. D. Zeh, C. Kiefer, D. Giulni, J. Kupsch, and I. O. Stamatescu, *Decoherence and the Appearance of a Classical World in Quantum Theory*, 2nd ed. (Springer, Berlin, 2003).

[5] H.-P. Breuer and F. Petruccione, *The Theory of Open Quantum Systems* (Oxford University Press, Oxford, 2002).

[6] P. C. E. Stamp, The decoherence puzzle, Studies Hist. Philos, Sci. Part B **37**, 467 (2006).

[7] A. Stern, Y. Aharonov, and Y. Imry, Phase uncertainty and loss of interference: A general picture, Phys. Rev. A **41**, 3436 (1990).

[8] L. H. Ford, Electromagnetic vacuum fluctuations and electron coherence, Phys. Rev. D **47**, 5571 (1993).

[9] H.-P. Breuer and F. Petruccione, Destruction of quantum coherence through emission of bremsstrahlung, Phys. Rev. A **63**, 032102 (2001).

[10] F. Bloch and A. Nordsieck, Note on the radiation field of the electron, Phys. Rev. **52**, 54 (1937).

[11] V. V. Sudakov, Vertex parts at very high energies in quantum electrodynamics, Zh. Eksp. Teor. Fiz. **30**, 87 (1956) [Sov. Phys.–JETP **3**, 65 (1956)].

[12] A. A. Abrikosov, The infrared catastrophe in quantum electrodynamics, Zh. Eksp. Teor. Fiz. **30**, 96 (1956) [Sov. Phys.–JETP **3**, 71 (1956)].

[13] T. Murota, On radiative corrections due to soft photons, Prog. Theor. Phys. **24**, 1109 (1960).

[14] T. Kinoshita, Note on the infrared catastrophe, Prog. Theor. Phys. **5**, 1045 (1950).

[15] N. Nakanishi, General theory of infrared divergence, Prog. Theor. Phys. **19**, 159 (1958).

[16] D. R. Yennie, S. C. Frautschi, and H. Suura, The infrared divergence phenomenon and high-energy processes, Ann. Phys. **13**, 379 (1961).

[17] T. Kinoshita, Mass singularities of Feynman amplitudes, J. Math. Phys. **3**, 650 (1962).

[18] G. Grammer and D. R. Yennie, improved treatment for the infrared divergence problem in Quantum Electrodynamics, Phys. Rev. D **8**, 4332 (1973).

[19] S. Weinberg, Infrared photons and gravitons, Phys. Rev. **140**, B516 (1965).

[20] T. He *et al.*, New symmetries of massless QED, J. High Energy Phys. 10 (2014) 112.

[21] D. Kapec *et al.*, New Symmetries of QED, Adv. Theor. Math. Phys. **21**, 1769 (2017).

[22] V. Lysov, S. Pasterski, and A. Strominger, Low's subleading soft theorem as a symmetry of QED, Phys. Rev. Lett. **113**, 111601 (2014).

[23] E. S. Fradkin, Application of functional methods in quantum field theory and quantum statistics. (I). Divergence-free field theory with local non-linear interaction, Nucl. Phys. **49**, 624 (1963).

[24] E. S. Fradkin, Application of functional methods in quantum field theory and quantum statistics. (II), Nucl. Phys. **76**, 588 (1966).

[25] J. Wilson-Gerow, C. DeLisle, and P. C. E. Stamp, A functional approach to soft graviton scattering and BMS charges, Class. Quantum Grav. **35**, 164001 (2018).

[26] V. Chung, Infrared divergence in quantum electrodynamics, Phys. Rev. **140**, B1110 (1965).

[27] T. W. B. Kibble, Coherent soft-photon states and infrared divergences. I. classical currents, J. Math. Phys **9**, 315 (1968).

[28] T. W. B. Kibble, Coherent soft-photon states and infrared divergences. II. mass shell singularities of Green's functions, Phys. Rev. **173**, 1527 (1968).

[29] T. W. B. Kibble, Coherent soft-photon states and infrared divergences. III. asymptotic states and reduction formulas, Phys. Rev. **174**, 1882 (1968).

[30] T. W. B. Kibble, Coherent soft-photon states and infrared divergences. IV. the scattering operator, Phys. Rev. **175**, 1624 (1968).

[31] P. P. Kulish and L. D. Faddeev, Asymptotic conditions and infrared divergences in quantum electrodynamics, Theor. Math. Phys. **4**, 745 (1971).

[32] D. Carney, L. Chaurette, D. Neuenfeld, and G. Semenoff, On the need for soft dressing, J. High Energy Phys. 09 (2018) 121.

[33] G. W. Semenoff, *Entanglement and the Infrared, in Lie Theory and Its Applications in Physics*, LT 2019, Springer Proceedings in Mathematics & Statistics, edited by V. Dobrev, Vol. 335 (Springer, Singapore, 2020).

[34] F. E. Low, Scattering of light of very low frequency by systems of spin 1/2, Phys. Rev. **96**, 1428 (1954).

[35] F. E. Low, Bremsstrahlung of very low-energy quanta in elementary particle collisions, Phys. Rev. **110**, 974 (1958).

[36] T. H. Burnett and N. M. Kroll, Extension of the low soft-photon theorem, Phys. Rev. Lett. **20**, 86 (1968).

[37] M. Gell-Mann and M. L. Goldberger, Scattering of low-energy photons by particles of spin 1/2, Phys. Rev. **96**, 1433 (1954).

[38] M. Campiglia and A. Laddha, Subleading soft photons and large gauge transformations, J. High Energy Phys. 11 (2016) 012.

[39] S. Choi and R. Akhoury, Subleading soft dressings of asymptotic states in QED and perturbative quantum gravity, J. High Energy Phys. 09 (2019) 031.

[40] D. Kapec, M. Perry, A.-M. Raclariu, and A. Strominger, Infrared divergences in QED, revisited, Phys. Rev. D **96**, 085002 (2017).

[41] C. DeLisle, J. Wilson-Gerow, and P. C. E. Stamp, Soft theorems from boundary terms in the classical point particle currents, J. High Energy Phys. 03 (2021) 290.

[42] S. W. Hawking, M. J. Perry, and A. Strominger, Soft hair on black holes, Phys. Rev. Lett. **116**, 231301 (2016).

[43] See, e.g., K. Hornberger, J. E. Sipe, and M. Arndt, Theory of decoherence in a matter wave Talbot-Lau interferometer, Phys. Rev. A **70**, 053608 (2004).

[44] N. V. Prokof'ev and P. C. E. Stamp, Theory of the spin bath, Rep. Prog. Phys. **63**, 669 (2000).

[45] G. Grynberg, A. Aspect, and C. Fabre, *Introduction to Quantum Optics* (Cambridge University Press, Cambridge, 2010).

[46] W. K. Wootters and W. H. Zurek, Complementarity in the double-slit experiment: Quantum nonseparability and a quantitative statement of Bohr's principle, Phys. Rev. D **19**, 473 (1979).

[47] D. M. Greenberger and A. Yasin, Simultaneous wave and particle knowledge in a neutron interferometer, Phys. Lett. A **128**, 391 (1988).

[48] B. G. Englert, Fringe visibility and which-way information: an inequality, Phys. Rev. Lett. **77**, 2154 (1996).

[49] T. Qureshi and R. Vathsan, Einstein's recoiling slit experiment, complementarity and uncertainty, Quanta **2**, 58 (2013).

[50] Decoherence functionals are described in, e.g., A. Schmid, On a quasiclassical Langevin equation, , J. Low Temp. Phys. **49**, 609 (1982).

[51] R. P. Feynman and F. L. Vernon, Theory of a general quantum system interacting with a linear dissipative system, Ann. Phys. **24**, 118 (1963).

[52] R. P. Feynman and A. R. Hibbs, *Quantum Mechanics and Path Integrals* (Dover, New York, 1965).

[53] V. Dinu, T. Heinzl, and A. Ilderton, Infrared divergences in plane wave backgrounds, Phys. Rev. D **86**, 085037 (2012).

[54] A. Laddha and A. Sen, Logarithmic terms in the soft expansion in four dimensions, J. High Energy Phys. 10 (2018) 056.

[55] J. D. Jackson, *Classical Electrodynamics*, 3rd ed. (Wiley, New York, 1999).

[56] D. Neuenfeld, Infrared-safe scattering without photon vacuum transitions and time-dependent decoherence, J. High Energy Phys. 11 (2021) 189.

[57] P. W. Anderson, B. I. Halperin, and C. M. Varma, Anomalous low-temperature properties of glasses and spin glasses, Philos. Mag. **25**, 1 (1972)

[58] For patch potentials, see M. Brownnutt, M. Kumph, P. Rabl, and R. Blatt, Ion-trap measurements of electric-field noise near surfaces, Rev. Mod. Phys. **87**, 1419 (2015); for the effecton Casimir measurements, see J. L. Garrett, J. Kim, and J. M. Munday, Measuring the effect of electrostatic patch potentials in Casimir force experiment, Phys. Rev. Res. **2**, 023355 (2020).

[59] A. O. Caldeira and A. J. Leggett, Quantum tunneling in a dissipative system, Ann. Phys. **149**, 374 (1983).

[60] H. Batelaan, E. Jones, W. C.-W. Huang, and R. Bach, Momentum Exchange in the electron double-slit experiment, J. Phys.: Conf. Ser. **701**, 012007 (2016).

[61] P. M. Echenique, R. H. Ritchie, N. Barbaran, and J. Inkson, Semiclassical image potential at a charged surface, Phys. Rev. B **23**, 6486 (1981).

[62] T. Wessel-Berg, *Electromagnetic and Quantum Measurements: A Bitemporal Neoclassical Theory* (Springer, Berlin, 2001).

[63] For reviews of the Casimiar effect, see G. L. Klimchitskaya, U. Mohideen, and V. M. Mostapanenko, Casimir force between real materials: experiment and theory, Rev. Mod. Phys. **81**, 1827 (2009); A. Lambrecht and S. Reynaud, Casimir effect: theory and experiment, Int. J. Mod. Phys. A **27**, 1260013 (2012).

[64] V. N. Popov, *Functional Integrals in Quantum Field Theory and Statistical Physics* (D. Reidel, Dordrecht, 1983).

[65] M. LeBellac, *Quantum and Statistical Field Theory* (Clarendon, Oxford, 1991).

[66] Y. Y. Fein, P. Geyer, P. Zwick, F. Kialka, S. Pedalino, M. Mayor, S. Gerlich, and M. Arndt, Quantum superposition of molecules beyiond 25 kDa, Nat. Phys. **15**, 1242 (2019).

[67] See G. L. Klimchitskaya *et al.*, Ref. [63].

[68] P. A. Maia Neto, A. Lambrecht, and S. Reynaud, Casimir energy between a plane and a sphere in electromagnetic vacuum, Phys. Rev. A **78**, 012115 (2008).

[69] S. J. Rahi, T. Emig, N. Graham, R. L. Jaffe, and M. Kardar, Scattering theory aproach to electrodynamic Casimir forces, Phys. Rev. D **80**, 085021 (2009).

[70] A. Canaguier-Durand, R. Guerout, P. A. M. Neto, A. Lambrecht, and S. Reynaud, The Casimir effect in the sphere-plane geometry, Int. J. Mod. Phys. Conf. Ser. **14**, 250 (2012).

[71] Van der Waals forces have been reviewed in, e.g., L. D. Landau and E. M. Lifshitz, *Electrodynamics of Continuous Media* (Pergamon, New York, 1960); J. N. Israelachvili, *Intermolecular and Surface Forces* (Academic, New York, 1992).

[72] P. W. Cleary, Elastoplastic deformation during projectile-wall collision, Appl. Math. Modell. **34**, 266 (2010).

[73] P. M. Echenique and J. B. Pendry, Reflectivity of liquid ^{4}He surfaces rti ^{4}He atoms, Phys. Rev. Lett. **37**, 561 (1976).

[74] D. R. Swanson and D. O. Edwards, Path-integral theory of the scattering of ^{4}He atoms at the surface of liquid ^{4}He, Phys. Rev. B **37**, 1539 (1988).

[75] J. Schwinger, L. L. DeRaad, K. A. Milton, and W. Y. Tsai, *Classical Electrodynamics* (Perseus Books, New York, 1998).

[76] Y. Luo, R. Zhao, and J. B. Pendry, van der Waals interactions at the nanoscale: the effects of nonlocality, Proc. Natl. Acad. Sci. USA **111**, 18422 (2014).

[77] V. Del Duca, High-energy bremsstrahlung theorems for soft photons, Nucl. Phys. B **345**, 369 (1990).

[78] Z. Bern, S. Davies, and J. Nohle, On loop corrections to subleading soft behavior of gluons and gravitons, Phys. Rev. D **90**, 085015 (2014).

[79] S. He, Y.-T. Huang, and C. Wen, Loop corrections to soft theorems in gauge theories and gravity, J. High Energy Phys. 12 (2014) 115.

[80] B. Sahoo and A. Sen, Classical and quantum results on logarithmic terms in the soft theorem in four dimensions, J. High Energy Phys. 02 (2019) 086.

[81] F. Cachazo and A. Strominger, Evidence for a new soft graviton theorem, arXiv:1404.4091.

[82] I. S. Gradshteyn and I. M. Ryzhik, *Table of Integrals, Series, and Products* (Academic, New York, 1980).